Supporting Information

Ferrocene - Diiron(I) Bis-Cyclopentadienyl Conjugates Exhibit Potent in Vitro Cytotoxicity and Selectivity Towards Cancer Cells Associated with ROS Scavenging

Chiara Saviozzi,[a] Lorenzo Biancalana,[a,*] Tarita Biver,[a] Tiziana Funaioli,[a] Marco Bortoluzzi,[b] Stefano Zacchini,[c] Krzysztof Krawczyk,[d] Andrzej Błauż,[d] Błażej Rychlik,[d,*] Fabio Marchetti[a,*]

[a] Department of Chemistry and Industrial Chemistry, University of Pisa, Via Giuseppe Moruzzi 13, I-56124 Pisa, Italy

[d] Department of Molecular Sciences and Nanosystems, Ca' Foscari University of Venice, I-30175 Mestre, Venezia, Italy

[c] Department of Industrial Chemistry "Toso Montanari", University of Bologna, Via Piero Gobetti 85, 40129 Bologna, Italy

[d] Centre for Digital Biology and Biomedical Science – Biobank® Lodz, Faculty of Biology and Environmental Protection, University of Lodz, Pomorska 141/143, 90-236 Lodz, Poland

*Email addresses:

lorenzo.biancalana@unipi.it; blazej.rychlik@biol.uni.lodz.pl, fabio.marchetti@unipi.it

Table of contents	**Pages**
IR and NMR spectra of diiron compounds (**Figures S1-S36**)	S3-S23
qNMR purity assessment (**Figures S37-S42, Table S1**)	S24-S30
X-ray crystallography (**Tables S2-S3**)	S31
Simulated IR and NMR spectra (**Figures S43-S46**)	S32-S35
Cyclic voltammetry (**Figures S47-S48**)	S36
Cytotoxicity studies (**Figures S49-S50**)	S37-S38

IR and NMR spectra of diiron compounds

Figure S1. ^{1}H NMR spectrum (401 MHz, acetone-d_6) of **2** (*cis-E*/*cis-Z*/*trans-E*/*trans-Z* ratios = 4.3:2.3:1.2:1.0).

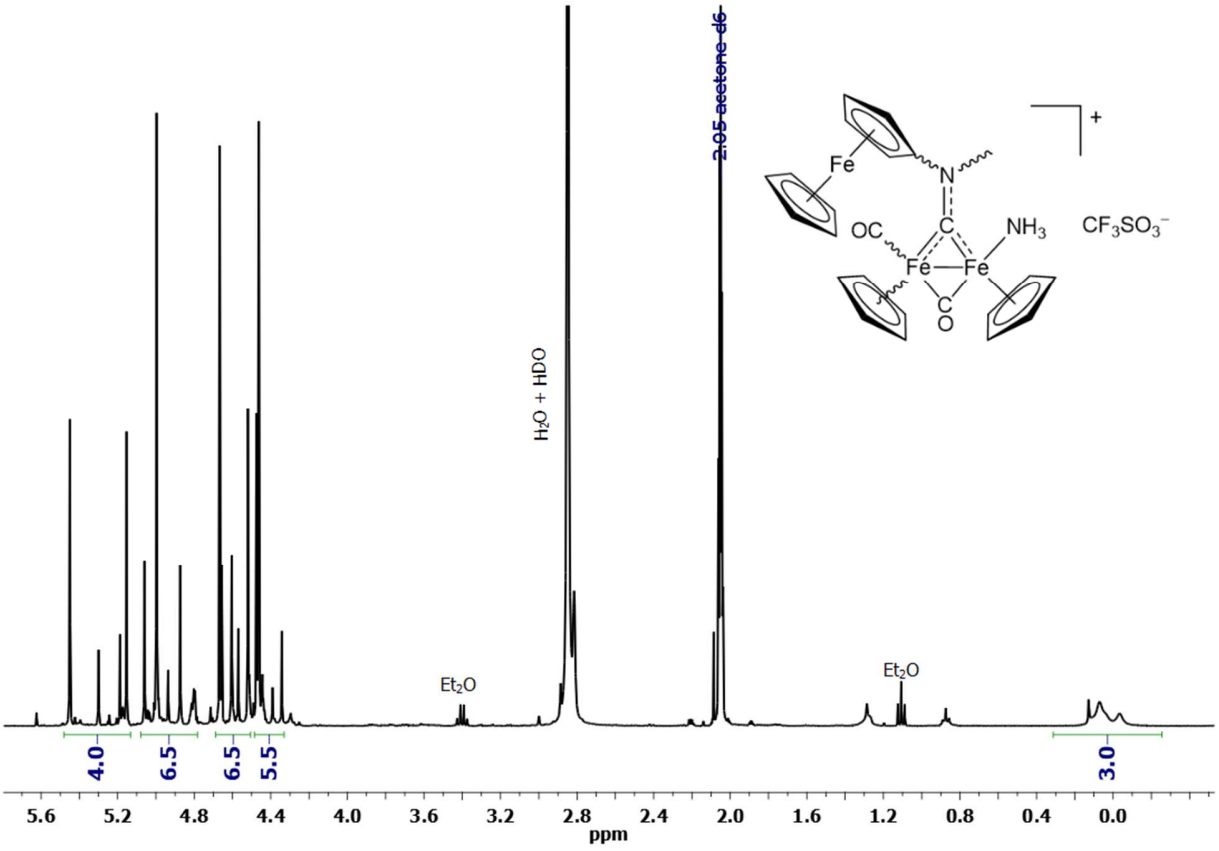

Figure S2. ^{1}H NMR spectrum (401 MHz, acetone-d_6) of **2**, highlighting the signals of the *cis-E* isomer.

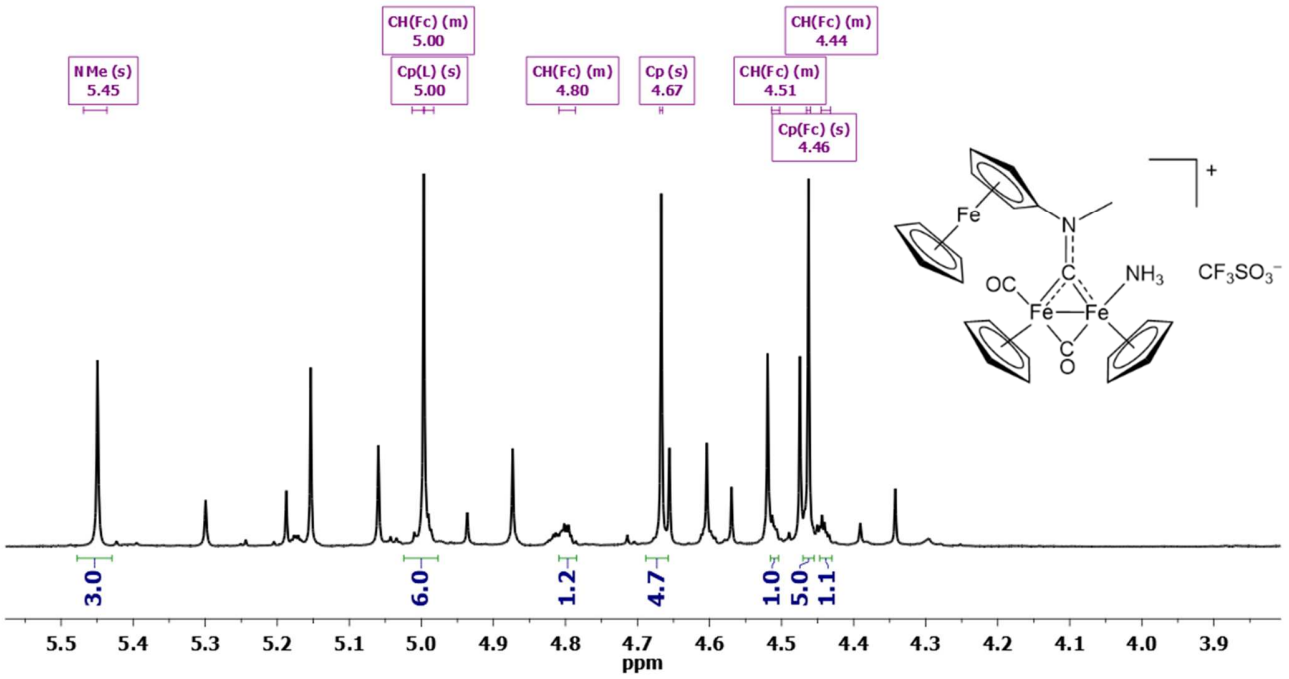

Figure S3. ^{1}H NMR spectrum (401 MHz, acetone-d_6) of **2**, highlighting the signals of the *cis*-Z isomer.

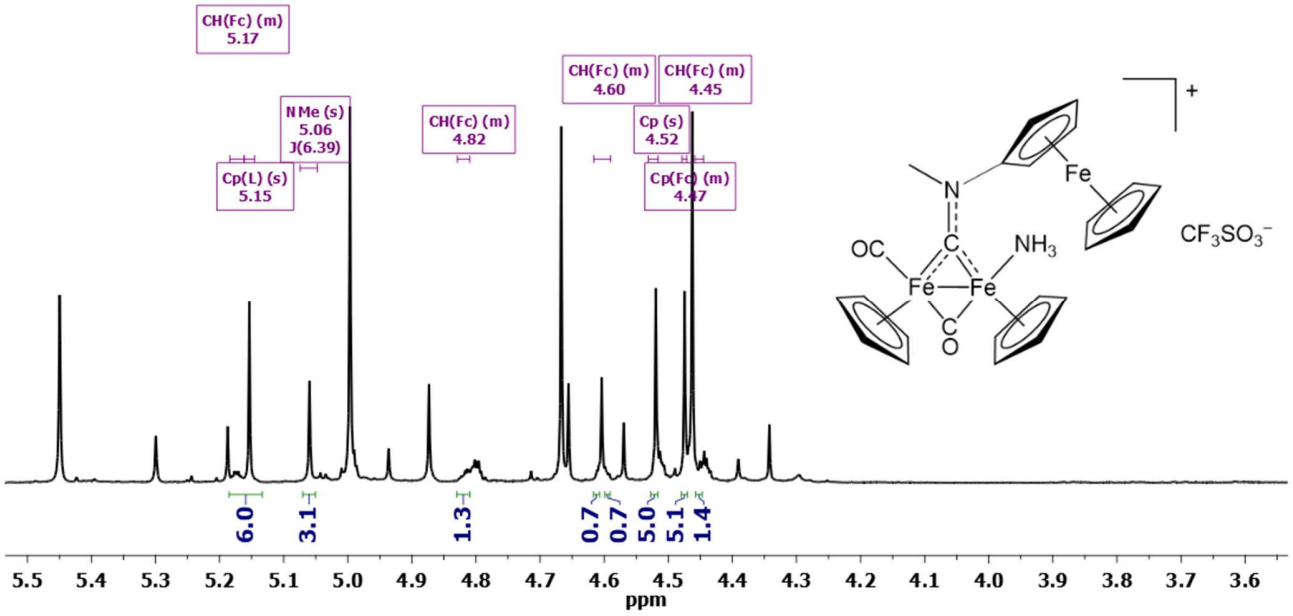

Figure S4. ^{1}H NMR spectrum (401 MHz, acetone-d_6) of **2**, highlighting the signals of the *trans-E* isomer.

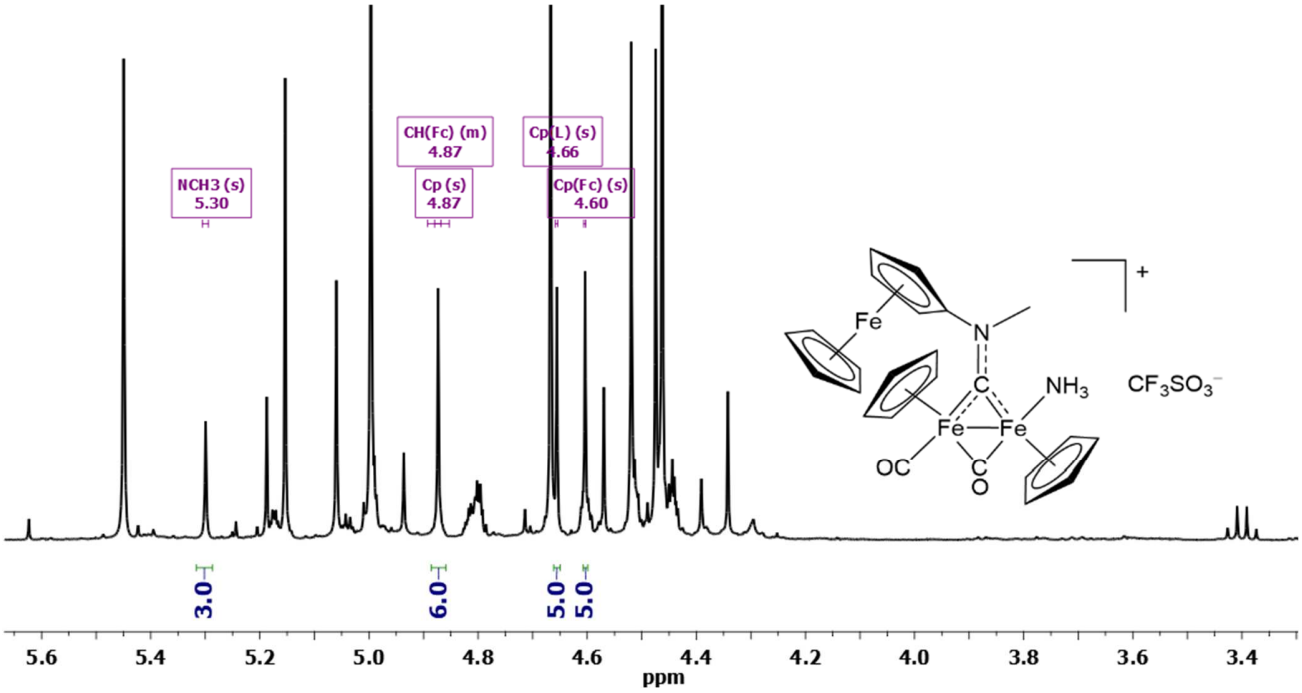

Figure S5. ^{1}H NMR spectrum (401 MHz, acetone-d_6) of **2**, highlighting the signals of the *trans-Z* isomer.

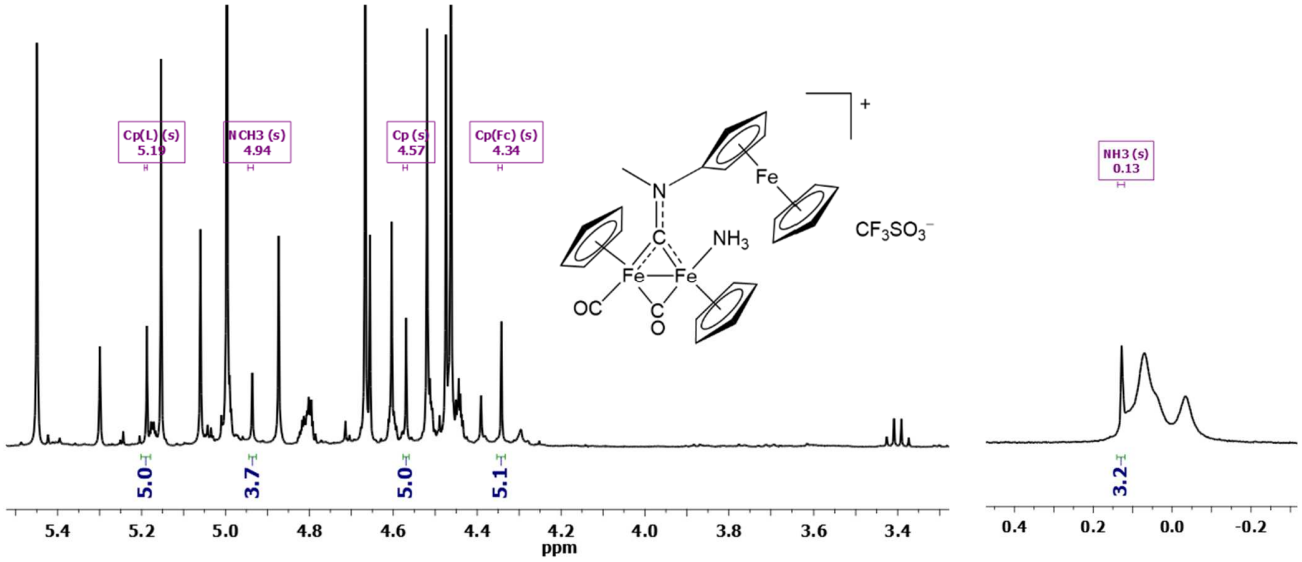

Figure S6. Black line: ^{1}H NMR spectrum (401 MHz, acetone-d_6) of **2**. Blue line: ^{1}H NOESY with irradiation at 4.67 ppm (Cp) of the *cis-E* isomer. Red line: ^{1}H NOESY with irradiation at 5.45 ppm (NCH_3) of the *cis-E* isomer. NOEs are indicated by the arrows.

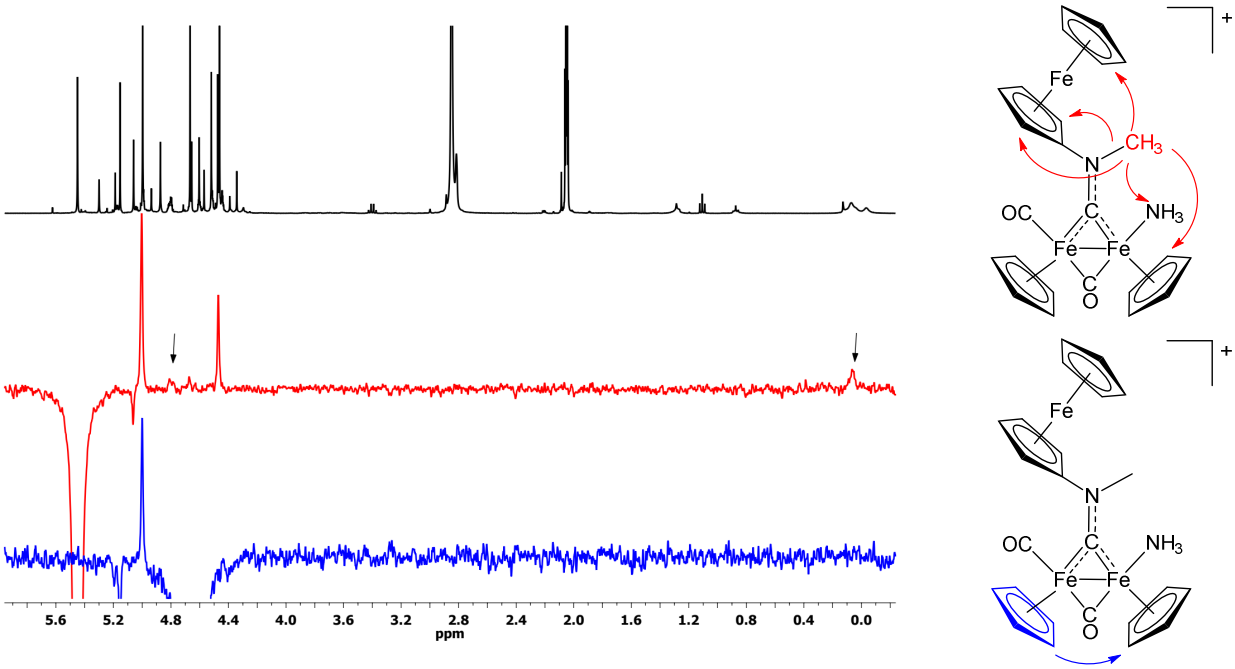

Figure S7. Black line: ^{1}H NMR spectrum (401 MHz, acetone-d_6) of **2**. Purple line: ^{1}H NOESY with irradiation at 5.15 ppm (Cp) of the *cis-Z* isomer. Green line: ^{1}H NOESY with irradiation at 5.06 ppm (NCH_3) of the *cis-Z* isomer. NOEs are indicated by the arrows.

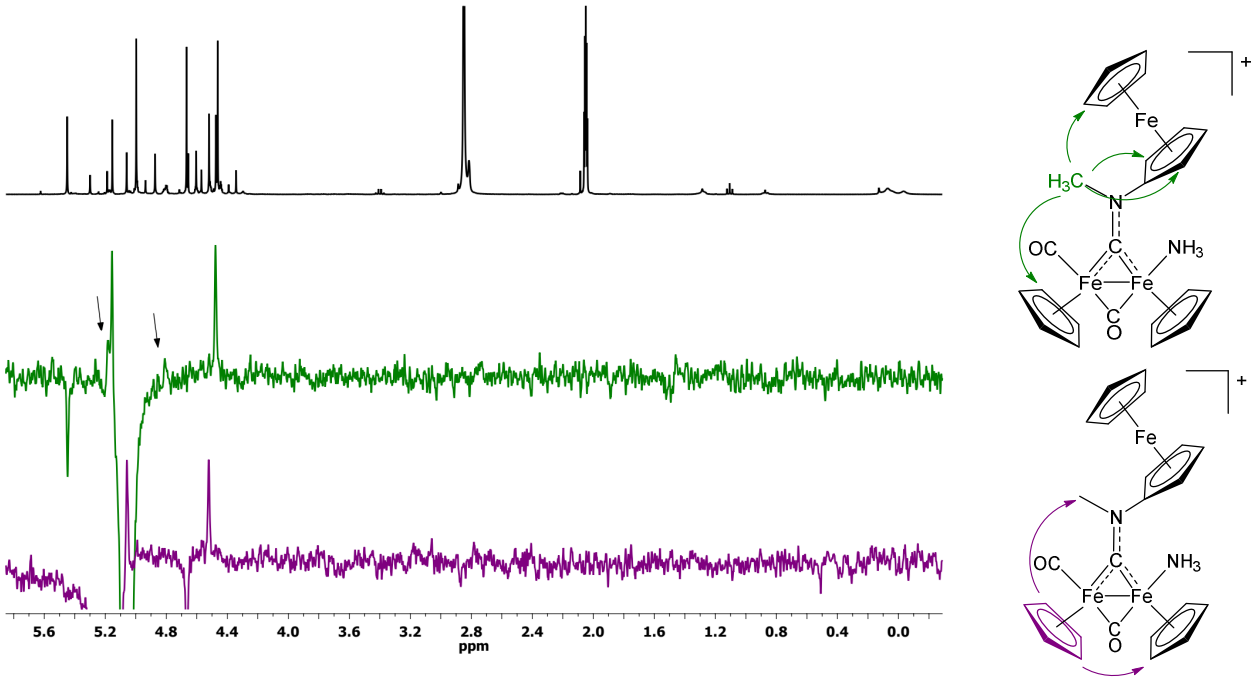

Figure S8. Black line: ^{1}H NMR spectrum (401 MHz, acetone-d_6) of **2**. Blue line: ^{1}H NOESY with irradiation at 4.67 ppm (Cp of the *cis-E* isomer). Purple line: ^{1}H NOESY with irradiation at 5.17 ppm (Cp of the *cis-Z* isomer). Red line: ^{1}H NOESY with irradiation at 5.45 ppm (NCH_3 of the *cis-E* isomer). Green line: ^{1}H NOESY with irradiation at 5.06 ppm (NCH_3 of the *cis-Z* isomer). Negative peaks (black arrows) indicate the chemical exchange underlying the partial magnetization transfer with the corresponding Cp ligand of the other diastereomer.

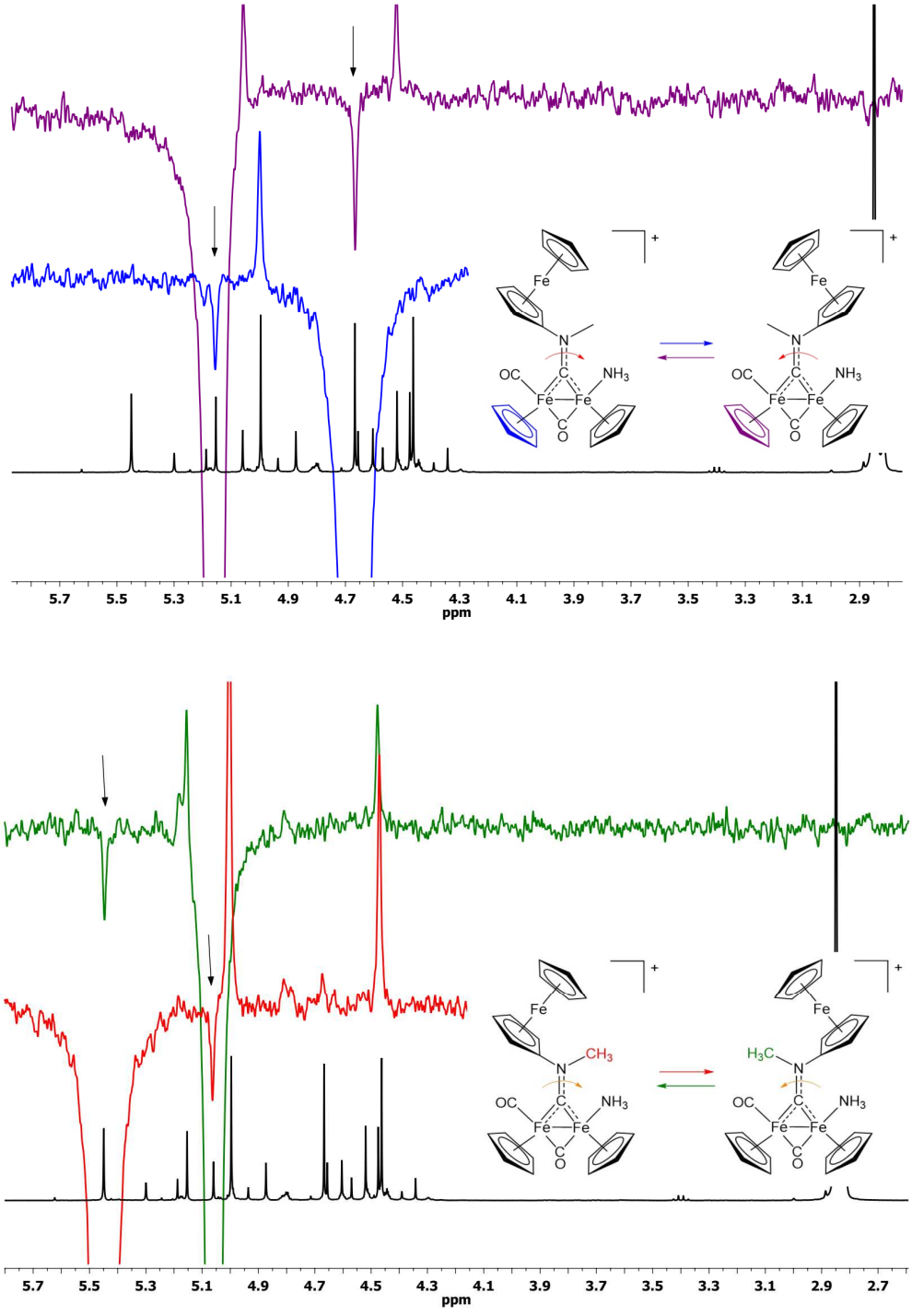

Figure S9. $^{13}C\{^1H\}$ NMR spectrum (101 MHz, acetone-d_6) of **2** (*cis-E/cis-Z*/*trans-E*/*trans-Z* ratios = 4.3:2.3:1.2:1.0). Only the resonances due to the major *cis-E*/*Z* isomers are highlighted.

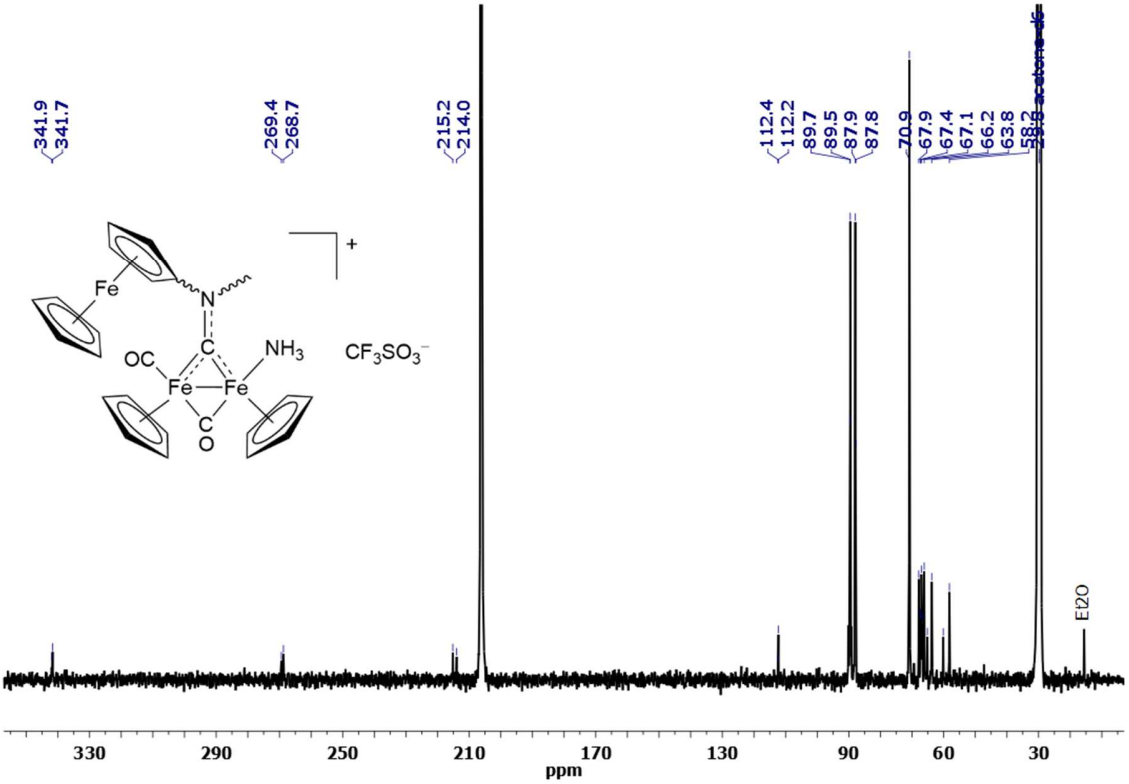

Figure S10. ^1H NMR spectrum (401 MHz, acetone-d_6) of $[Fe_2Cp_2(CO)_2(CNMe)\{\mu\text{-}CNMe(Fc)\}]CF_3SO_3$, **3a** (*cis-E/Z* ratio ≈ 1 + minor *trans-E*/*Z* isomers). Only the resonances due to the *cis-E*/*Z* isomers are highlighted.

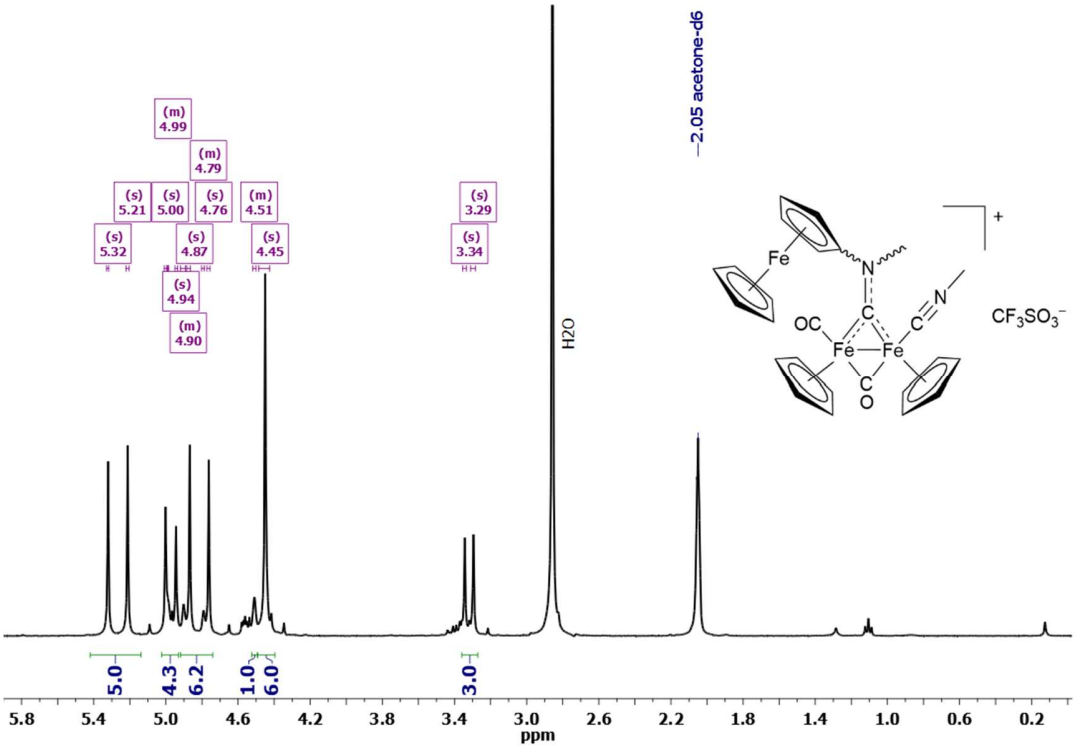

Figure S11. $^{13}C\{^{1}H\}$ NMR spectrum (101 MHz, acetone-d_6) of **3a** (*cis-E/Z* ratio ≈ 1 + minor *trans-E/Z* isomers). Only the resonances due to the *cis-E/Z* isomers are highlighted.

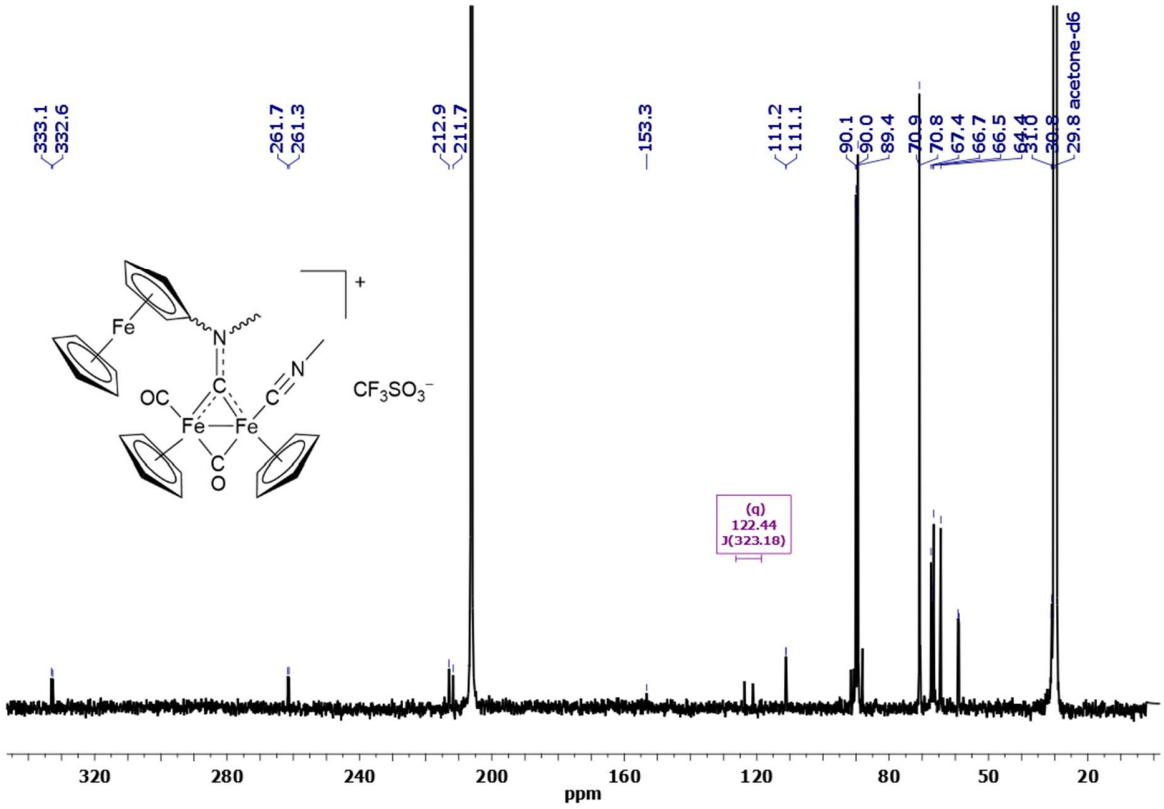

Figure S12. Solid-state IR spectrum (650-4000 cm^{-1}) of $[Fe_2Cp_2(CO)_2(CNCy)\{\mu\text{-}CNMe(Fc)\}]CF_3SO_3$, **3b** (mixture of *cis-E/Z* isomers).

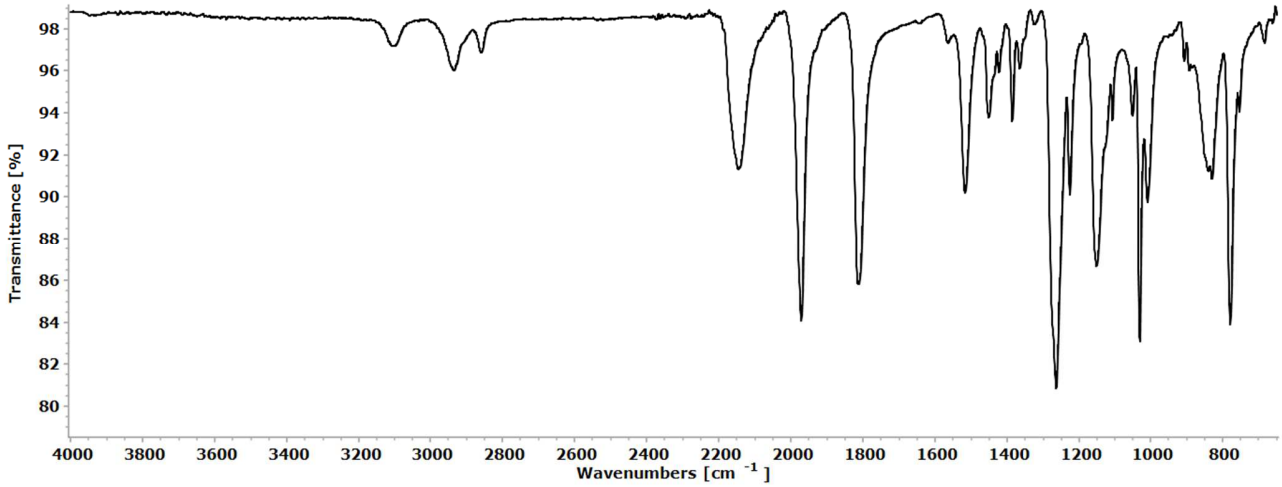

Figure S13. ^{1}H NMR spectrum (401 MHz, acetone-d_6) of **3b** (*cis-E/Z* ratio = 1.5).

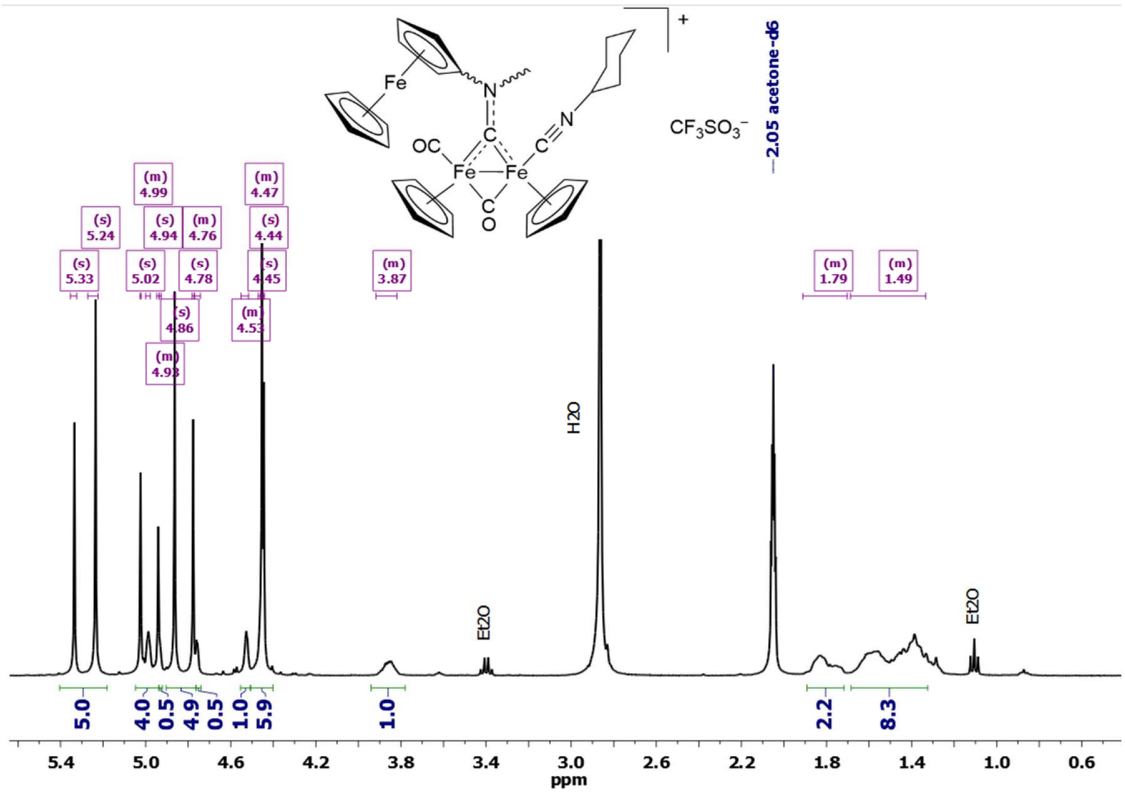

Figure S14. $^{13}C\{^{1}H\}$ NMR spectrum (101 MHz, acetone-d_6) of **3b** (*cis-E/Z* ratio = 1.5).

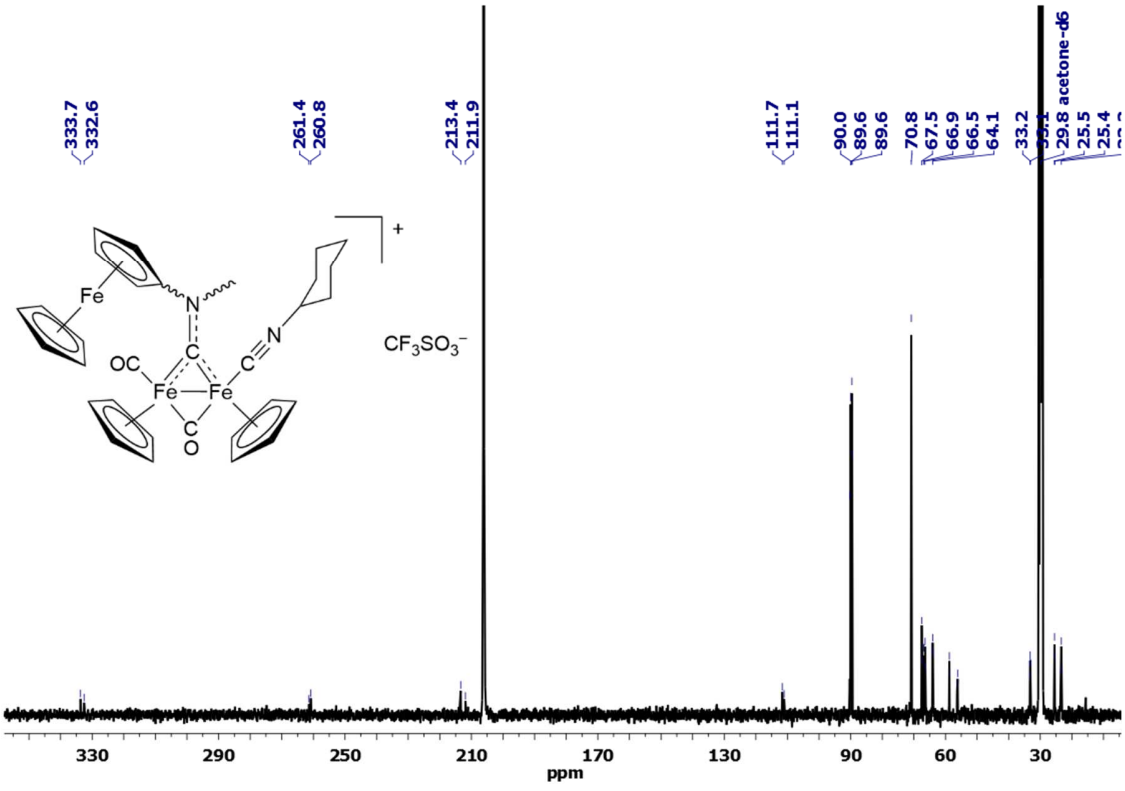

Figure S15. Black line: ^{1}H NMR spectrum (401 MHz, acetone-d_6) of **3b**. Blue line: ^{1}H NOESY with irradiation at 4.86 ppm (Cp of the *cis-E* isomer). Red line: ^{1}H NOESY with irradiation at 5.24 ppm (Cp^L of the *cis-E* isomer). Green line: ^{1}H NOESY with irradiation at 5.33 ppm (Cp of the *cis-Z* isomer). NOEs are indicated by the arrows.

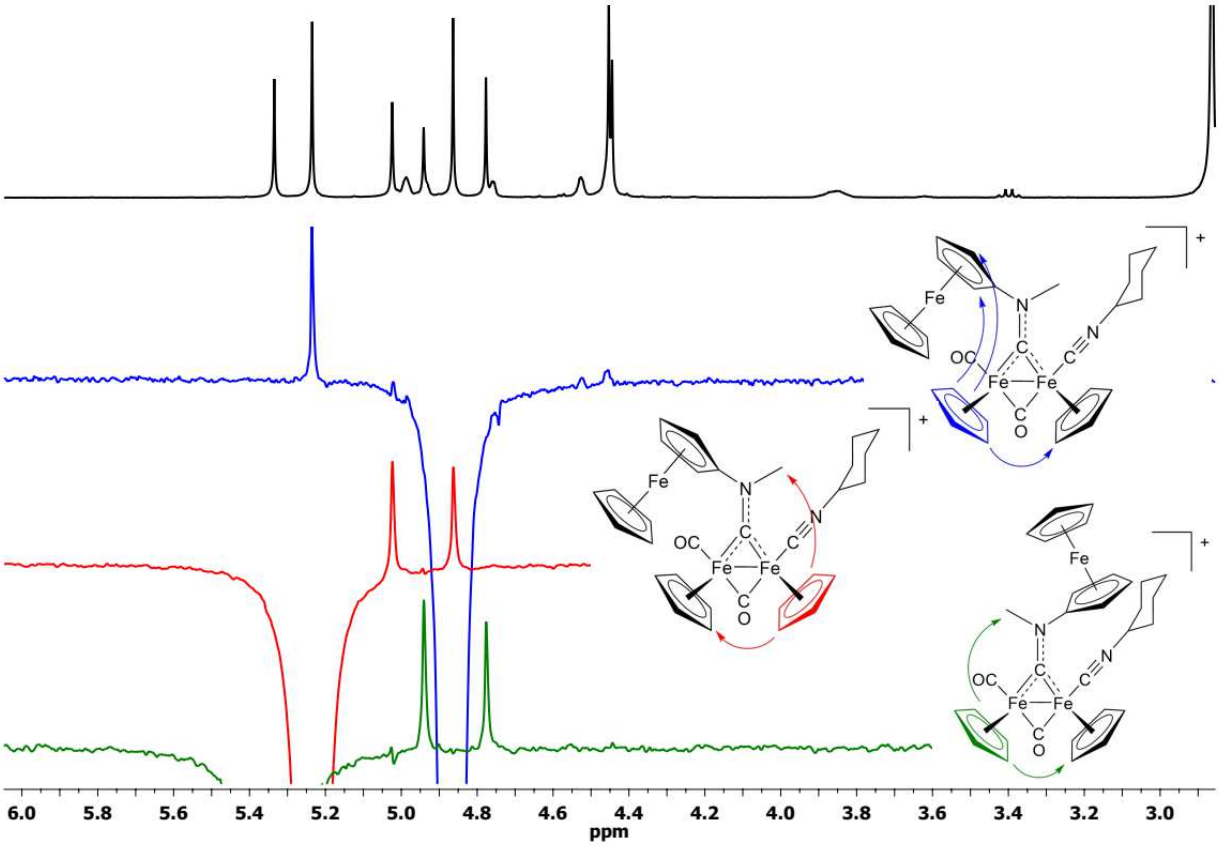

Figure S16. ^{1}H NMR spectrum (401 MHz, acetone-d_6) of $[Fe_2Cp_2(CNMe)_2(\mu\text{-}CO)\{\mu\text{-}CNMe(Fc)\}]CF_3SO_3$, **4a** (*trans*/*cis* ratio = 1.2). Signals due to the $[FeCp(CNMe)_3]^+$ by-product are marked with asterisk (*).

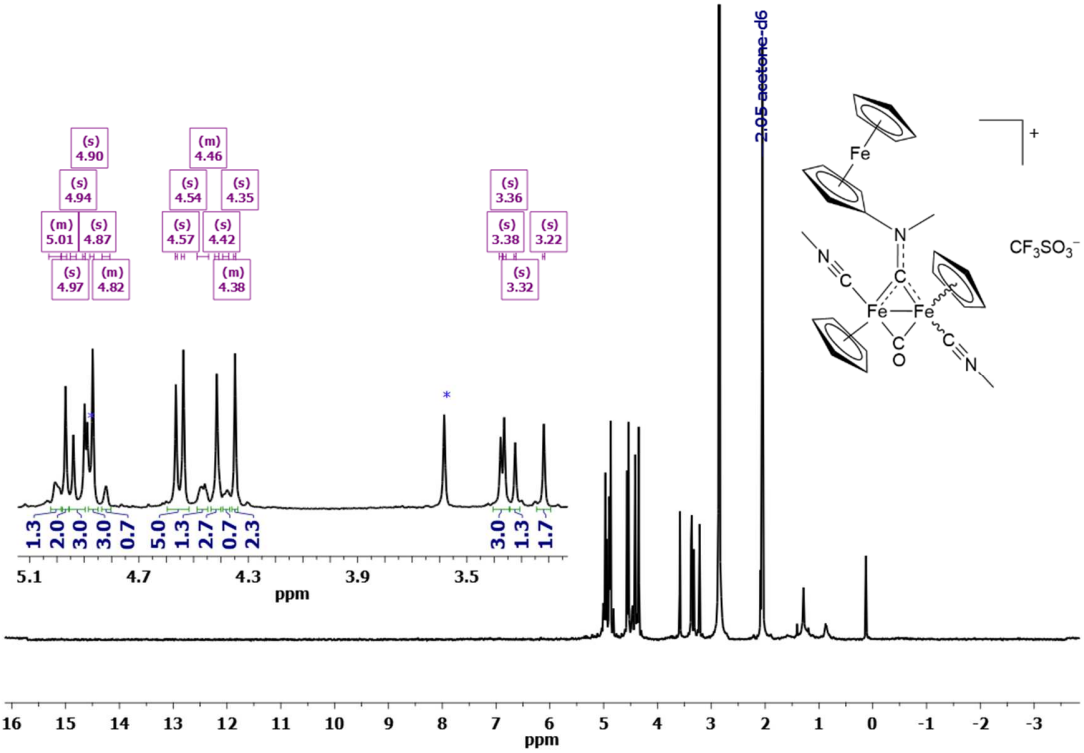

Figure S17. $^{13}C\{^{1}H\}$ NMR spectrum (101 MHz, acetone-d_6) of **4a** (*trans*/*cis* ratio = 1.2). Signals due to BHT (*) (2,6-di-tert-butyl-4-methylphenol, radical stabilizer present in commercial samples of THF) and the $[FeCp(CNMe)_3]^+$ byproduct (*) are marked with asterisks.

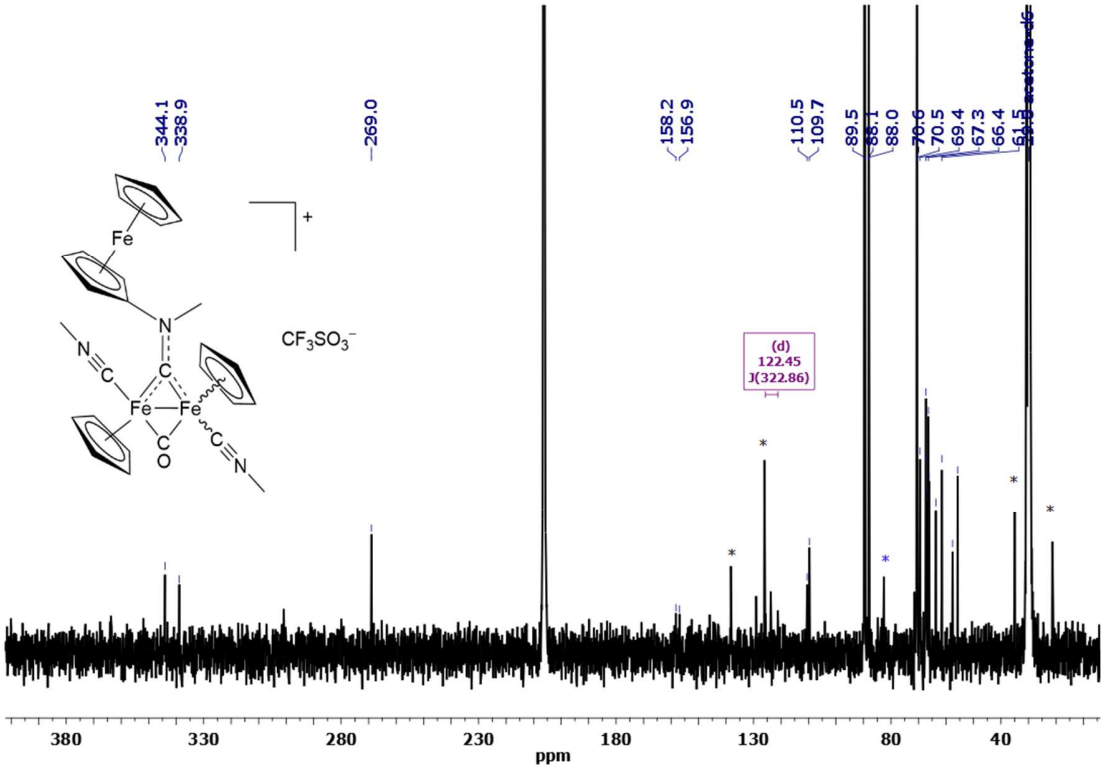

Figure S18. ^{1}H NMR spectrum (401 MHz, acetone-d_6) of $[Fe_2Cp_2(CNCy)_2(\mu\text{-}CO)\{\mu\text{-}CNMe(Fc)\}]CF_3SO_3$, **4b** (*trans*/*cis* ratio = 3). Signals due to the $[FeCp(CNCy)_3]^+$ by-product are marked with asterisk (*).

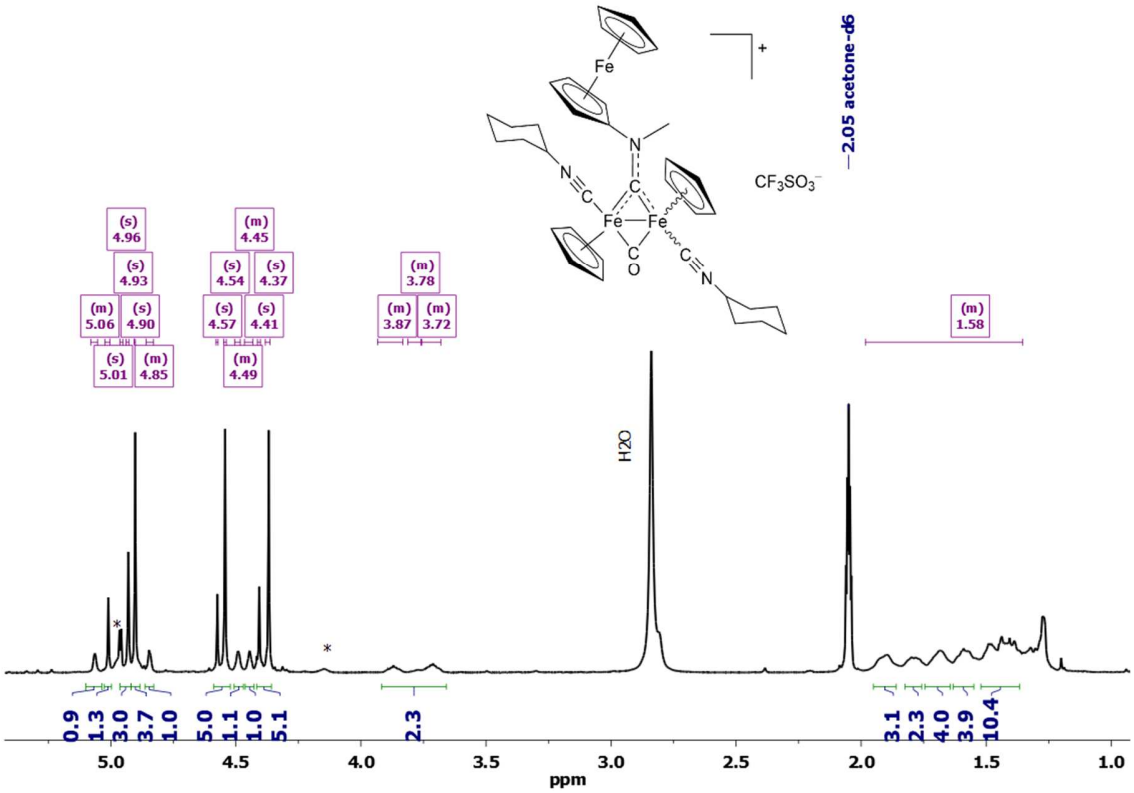

Figure S19. $^{13}C\{^{1}H\}$ NMR spectrum (101 MHz, acetone-d_6) of **4b** (*trans*/*cis* ratio = 3). Signals due to the $[FeCp(CNCy)_3]^+$ by-product are marked with asterisk (*).

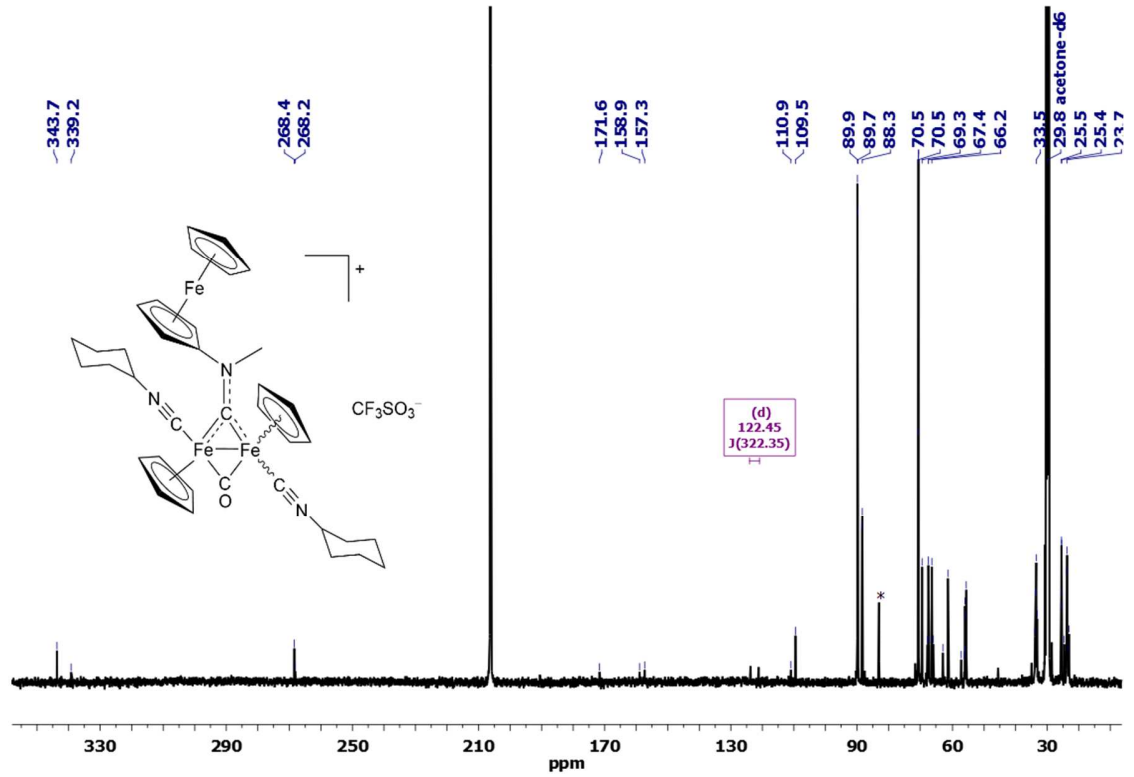

Figure S20. Black line: ^{1}H NMR spectrum (401 MHz, acetone-d_6) of **4b**. Red line: ^{1}H NOESY with irradiation at 5.01 ppm (Cp of the *cis* isomer). NOE is indicated by the arrow.

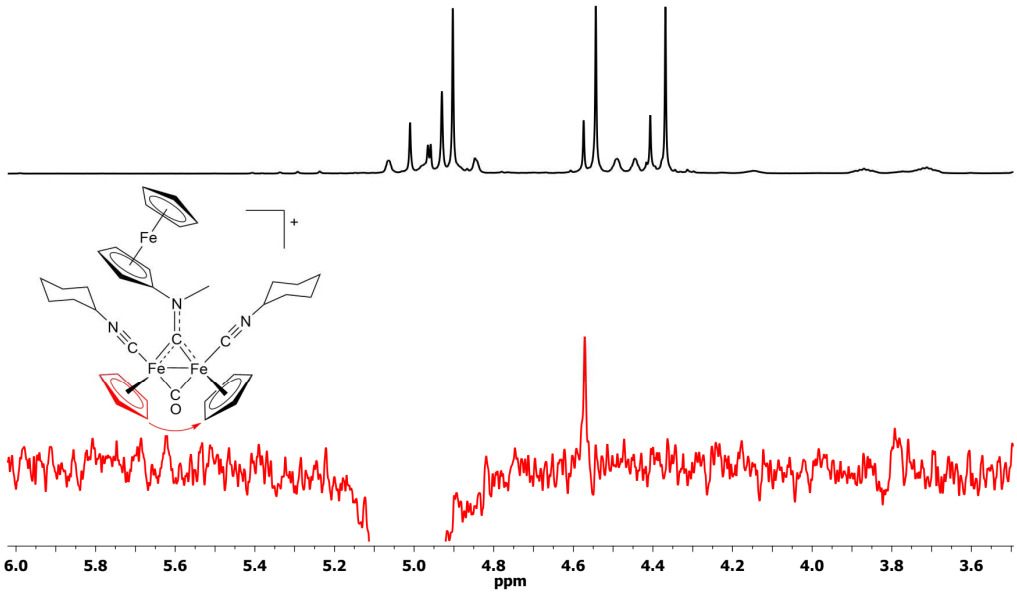

Figure S21. ^{1}H NMR spectrum (401 MHz, acetone-d_6) of $[Fe_2Cp_2\{CN(4\text{-}C_6H_4OMe)\}_2(\mu\text{-}CO)\{\mu\text{-}CNMe(Fc)\}]CF_3SO_3$, **4c** (*cis*/*trans* ratio = 1.5). Signals due to the $[FeCp\{CN(4\text{-}C_6H_4OMe)\}_3]^+$ by-product are marked with asterisk (*).

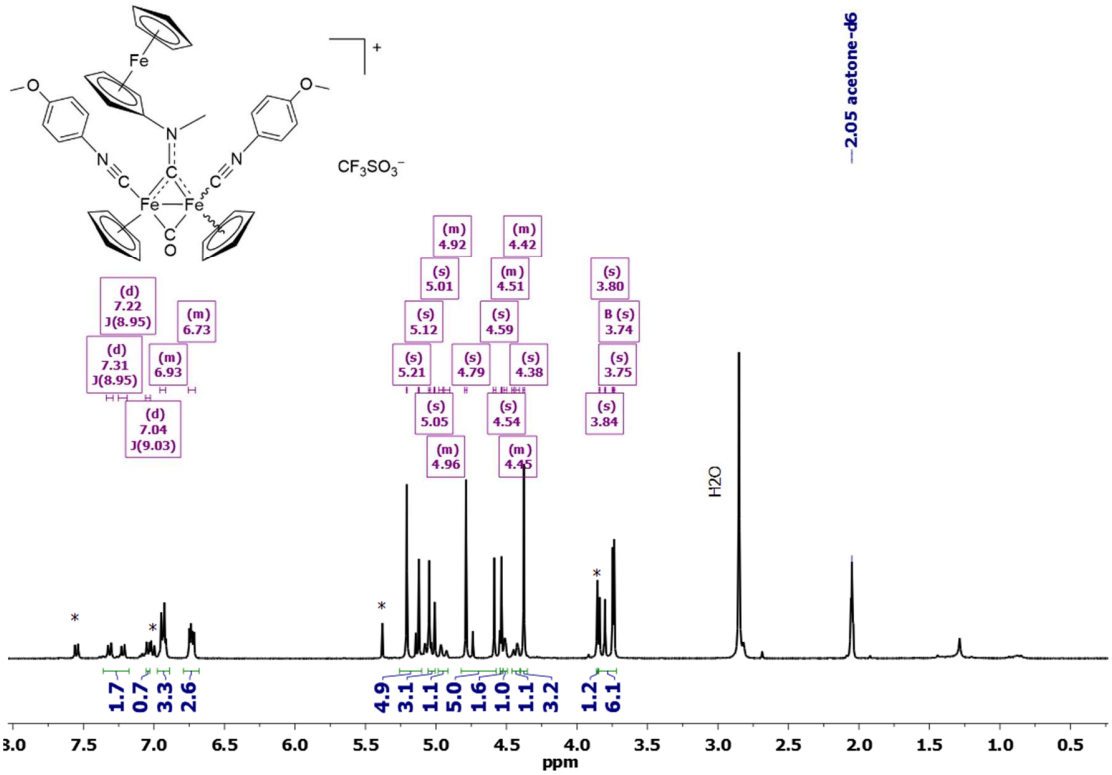

Figure S22. $^{13}C\{^{1}H\}$ NMR spectrum (101 MHz, acetone-d_6) of **4c** (*cis*/*trans* ratio = 1.5). Signals due to the $[FeCp\{CN(4\text{-}C_6H_4OMe)\}_3]^+$ by-product are marked with asterisk (*).

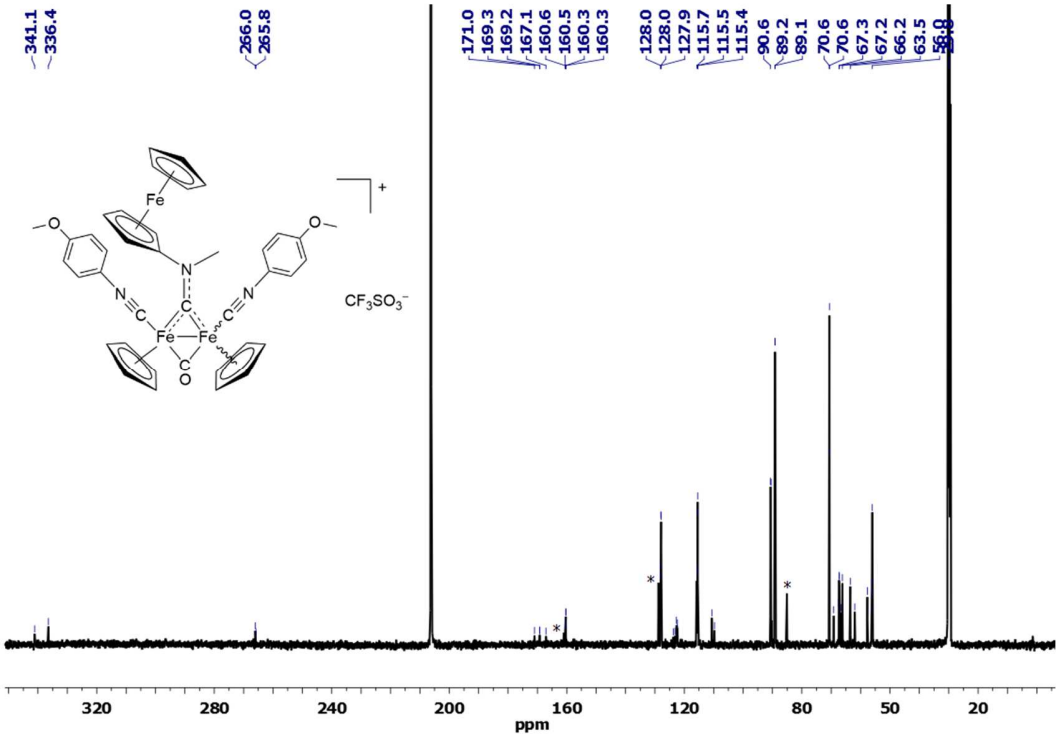

Figure S23. ^{1}H NOESY NMR spectra (401 MHz, acetone-d_6) of *trans*-**4c**. Blue line: irradiation at 5.12 ppm (Cp). Red line: irradiation at 4.59 ppm (Cp'). NOEs are indicated by the arrows; dotted lines indicate weak NOE effects.

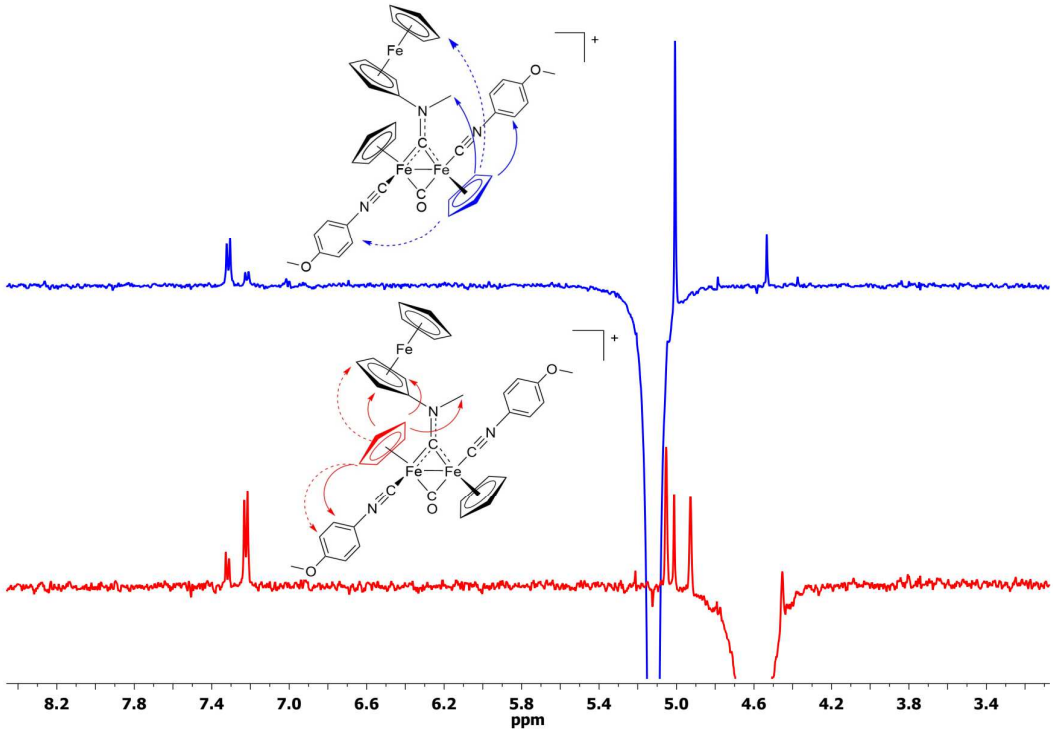

Figure S24. ^{1}H NOESY NMR spectra (401 MHz, acetone-d_6) of *cis*-**4c**. Blue line: irradiation at 5.21 ppm (Cp). Red line: irradiation at 4.79 ppm (Cp'). Green line: irradiation at 5.05 ppm (NCH_3). NOEs are indicated by the arrows; dotted lines indicate weak NOE effects.

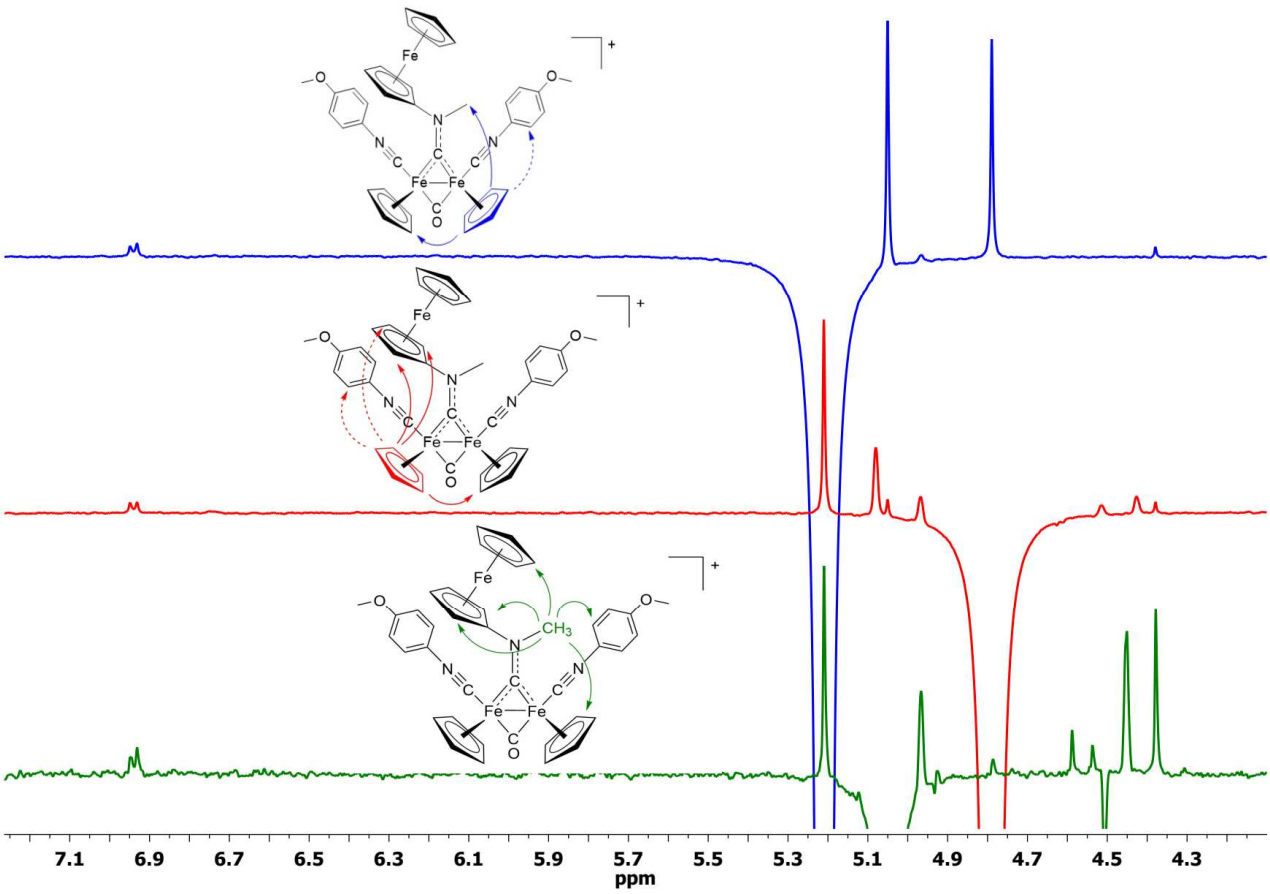

Figure S25. ^{1}H NMR spectrum (401 MHz, acetone-d_6) of $[Fe_2Cp_2(CO)(\mu\text{-}CO)\{\mu\text{-}\eta^1\text{:}\eta^3\text{-}C^3MeC^2HC^1NMe(Fc)\}]CF_3SO_3$, **5a** (*cis-E*/*Z* ratio = 2.5 + traces of *trans* isomers – not highlighted).

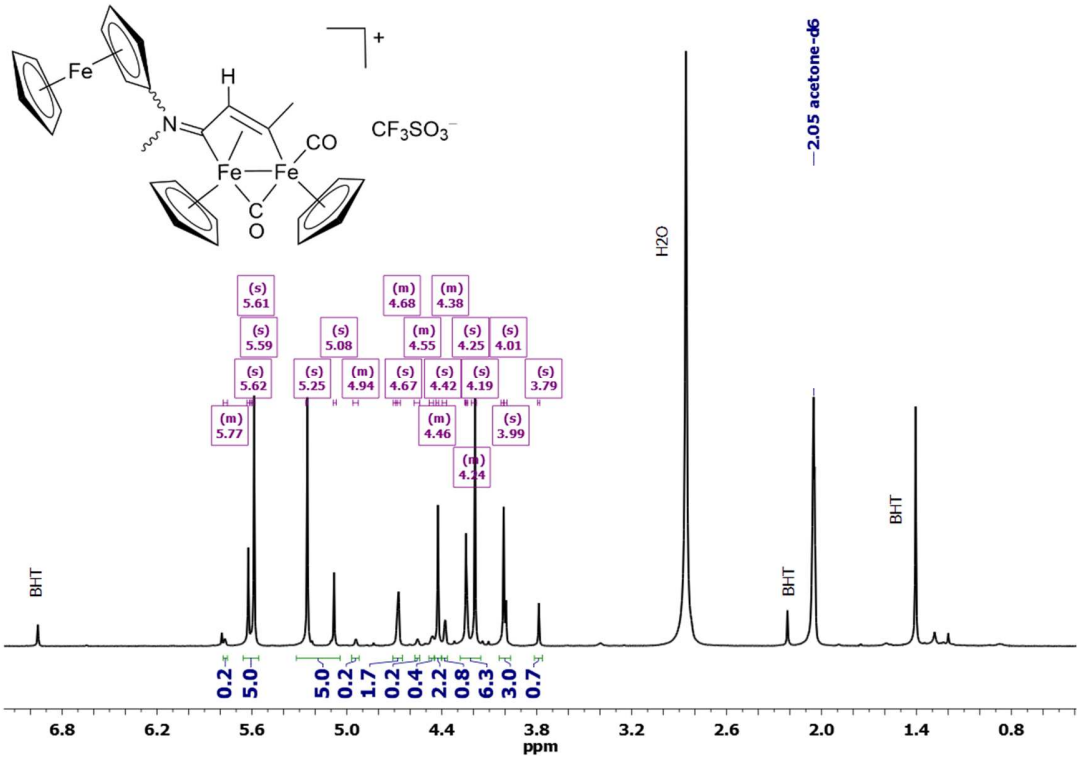

Figure S26. $^{13}C\{^{1}H\}$ NMR spectrum (101 MHz, acetone-d_6) of **5a** (*cis-E*/*Z* ratio = 2.5 + traces of *trans* isomers – not highlighted).

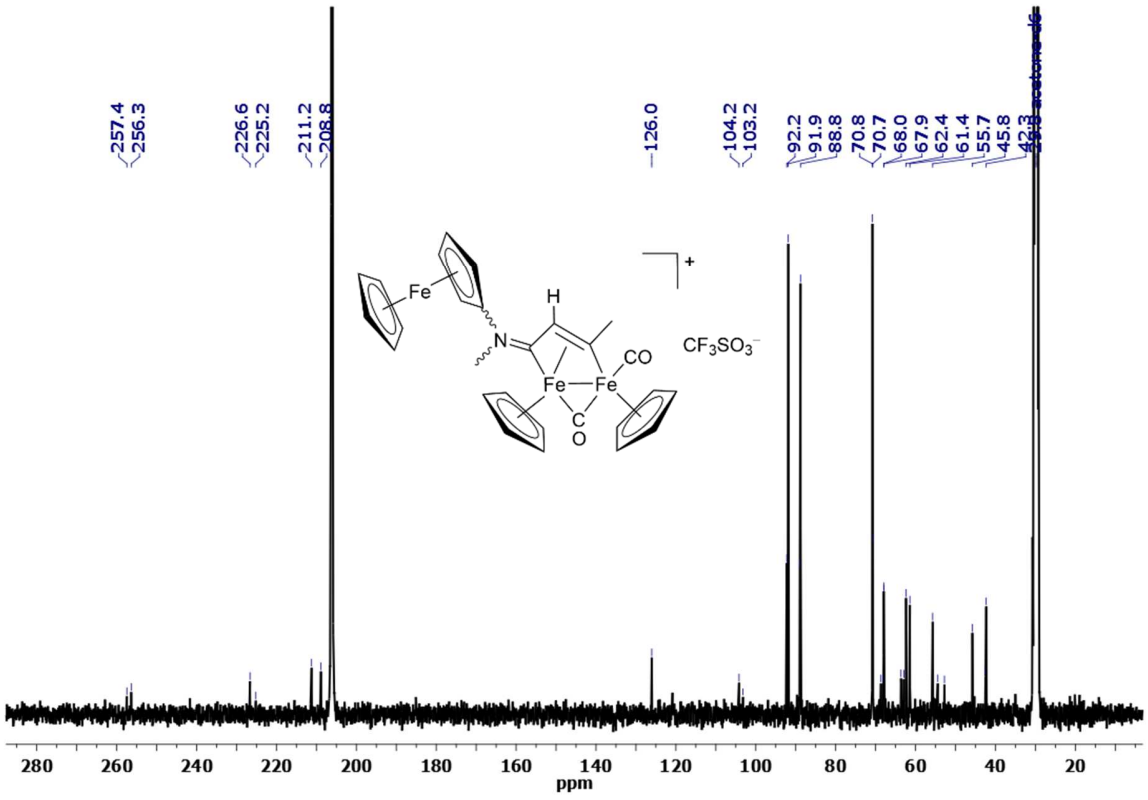

Figure S27. Black line: ^{1}H NMR spectrum (401 MHz, acetone-d_6) of **5a**. Blue line: ^{1}H NOESY with irradiation at 5.59 ppm (Cp) of the *cis-E* isomer. Red line: ^{1}H NOESY with irradiation at 5.25 ppm (Cp^L) of the *cis-E* isomer. Green line: ^{1}H NOESY with irradiation at 5.08 ppm (Cp^L) of the *cis-Z* isomer. NOEs are indicated by the arrows.

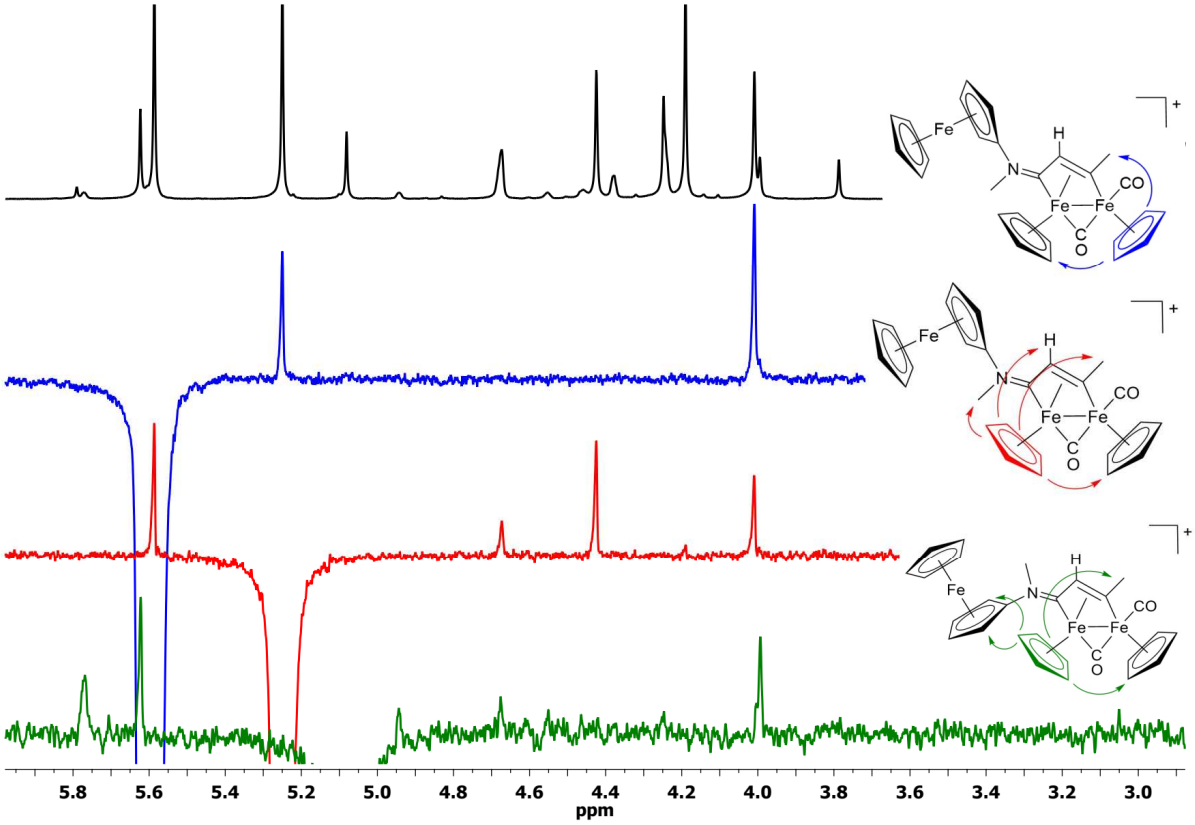

Figure S28. Solid-state IR spectrum (650-4000 cm^{-1}) of [$Fe_2Cp_2(CO)(\mu\text{-}CO)\{\mu\text{-}\eta^1\text{:}\eta^3\text{-}C^3PhC^2HC^1NMe(Fc)\}$]$CF_3SO_3$, *cis-E*-**5b**.

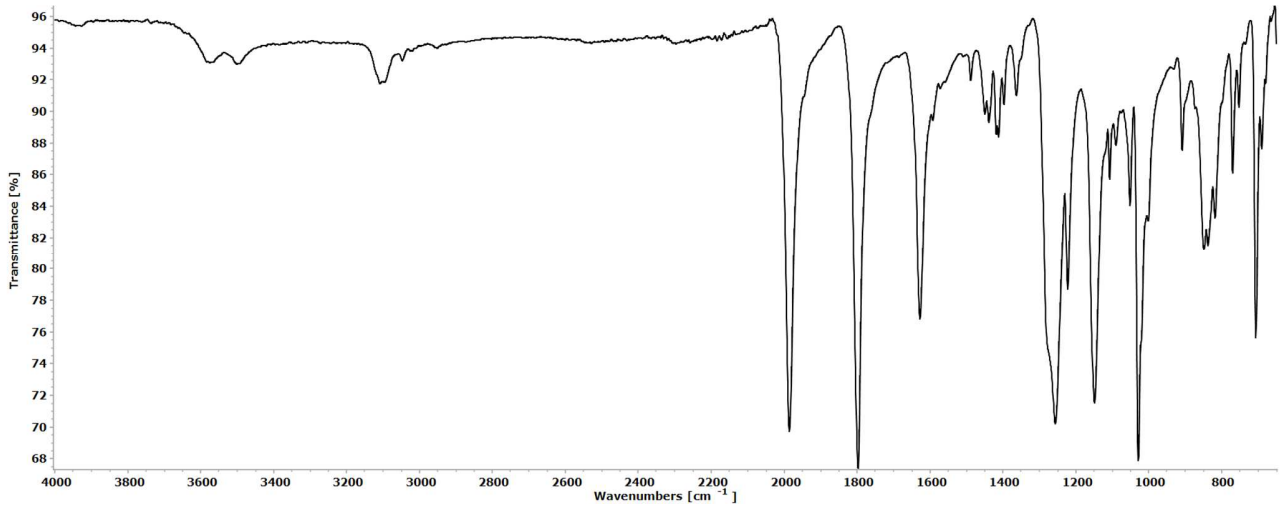

Figure S29. ^{1}H NMR spectrum (401 MHz, acetone-d_6) of *cis-E*-**5b**. Traces of *trans-E*-**5b** are indicated with the asterisk (*).

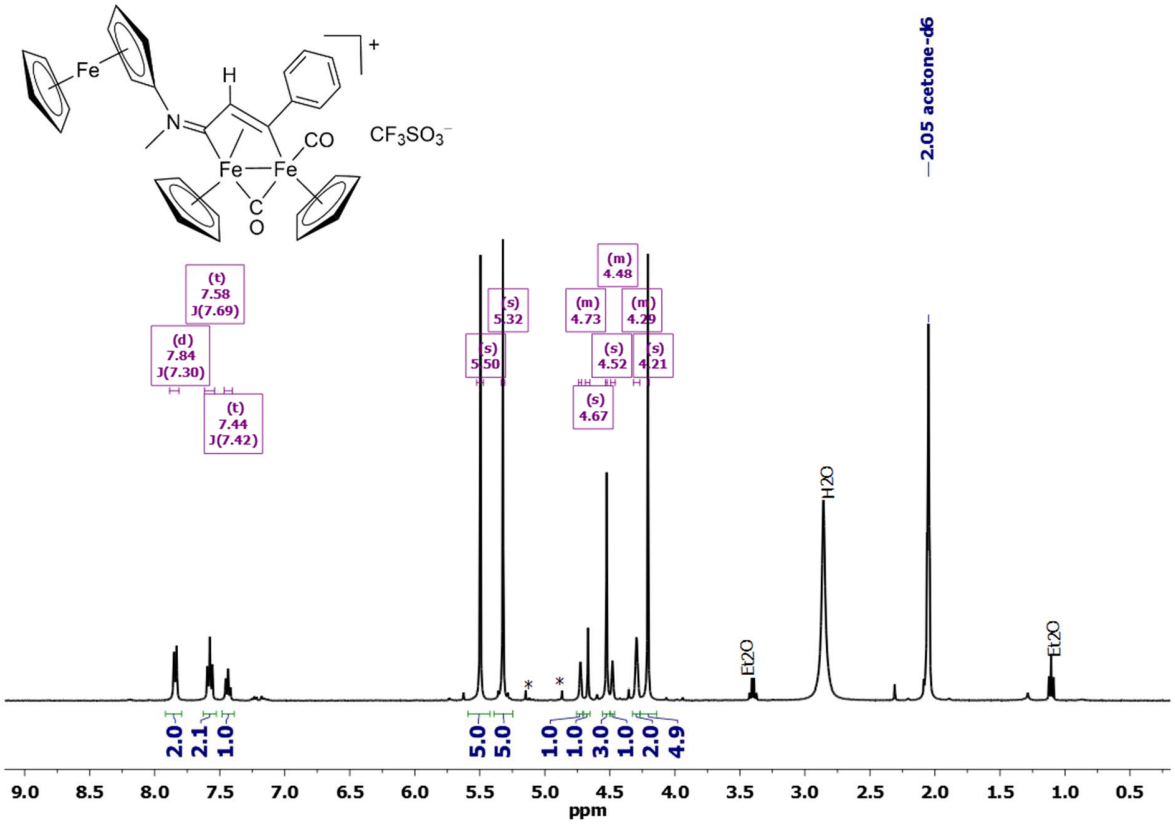

Figure S30. $^{13}C\{^{1}H\}$ NMR spectrum (101 MHz, acetone-d_6) of *cis-E*-**5b**.

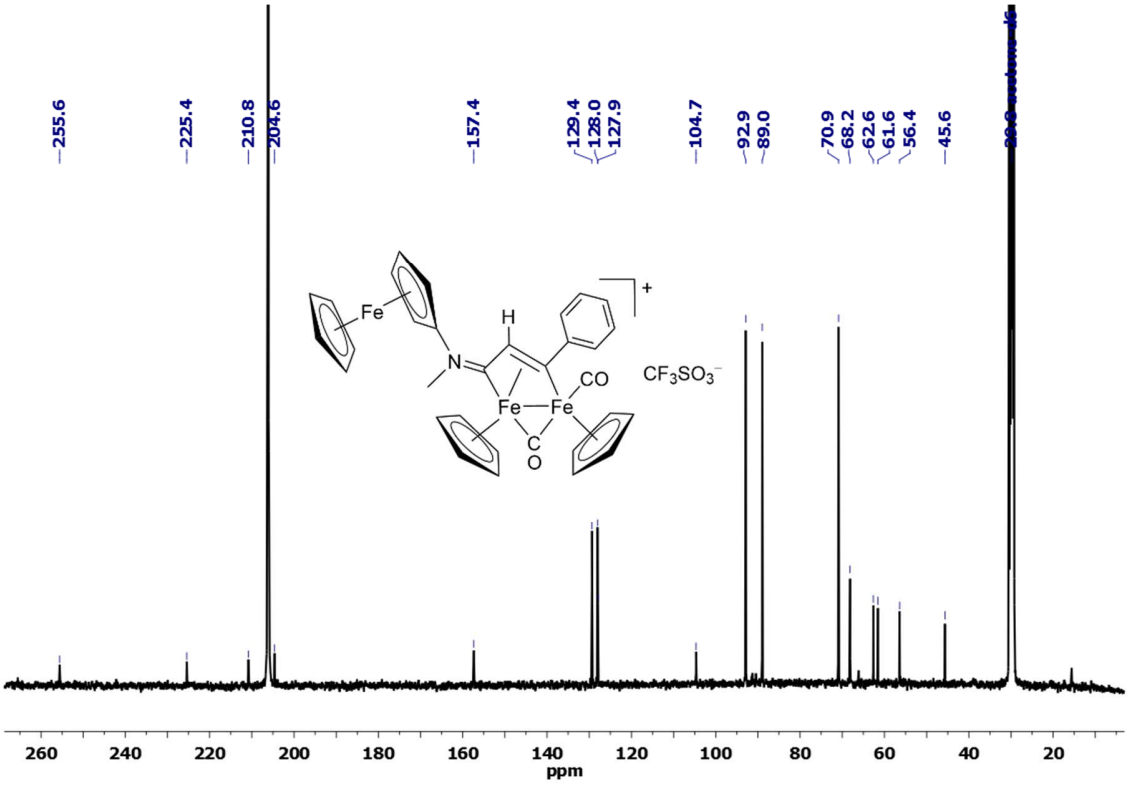

Figure S31. Black line: ^{1}H NMR spectrum (401 MHz, acetone-d_6) of *cis-E*-**5b**. Blue line: ^{1}H NOESY with irradiation at 5.50 ppm (Cp^L). Red line: ^{1}H NOESY with irradiation at 5.32 ppm (Cp). **A**: NOEs are indicated by the arrows. **B**: Negative peaks (black arrows) indicate the chemical exchange underlying the partial magnetization transfer with the corresponding Cp ligand of the *trans-E* diastereomer.

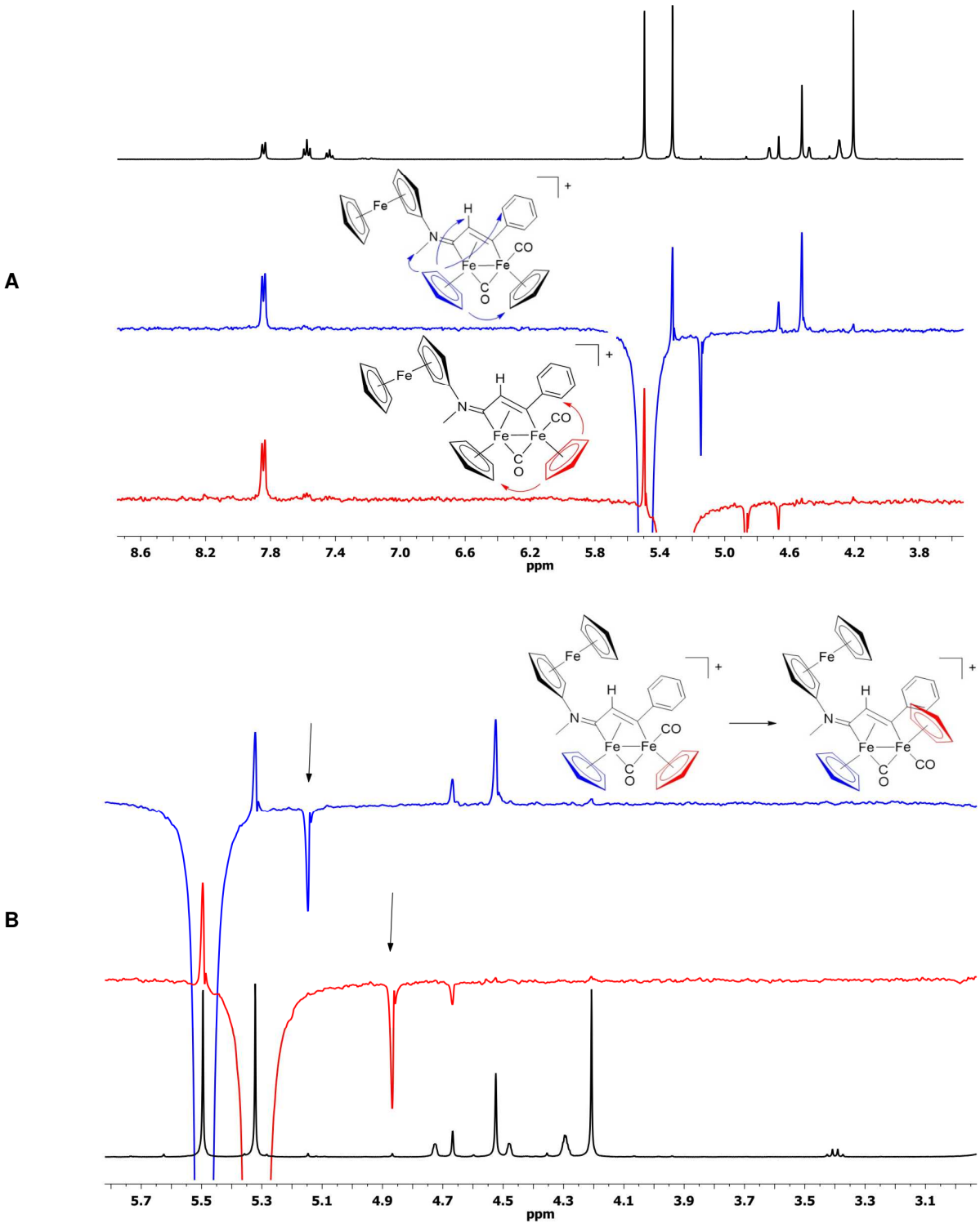

Figure S32. Solid-state IR spectrum (650-4000 cm^{-1}) of $[Fe_2Cp_2(CO)(\mu\text{-}CO)\{\mu\text{-}\eta^1\text{:}\eta^3\text{-}C^3MeC^2MeC^1NMe(Fc)\}]CF_3SO_3$, **5c** (mixture of *cis*-*E*/*Z* isomers).

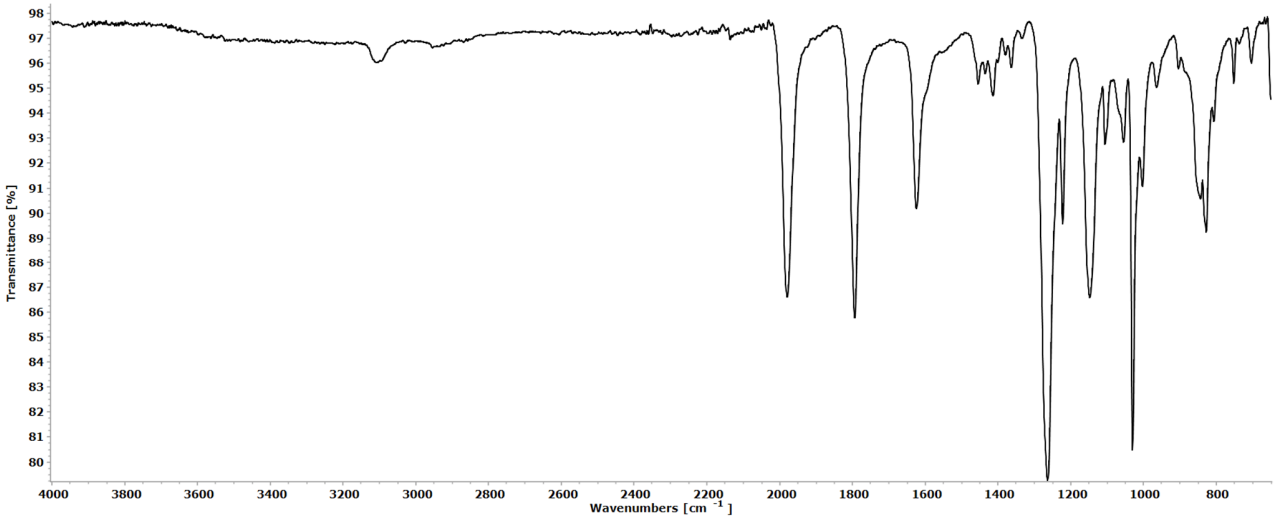

Figure S33. ^1H NMR spectrum (401 MHz, acetone-d_6) of **5c** (*cis*-*E*/*Z* ratio = 7.6).

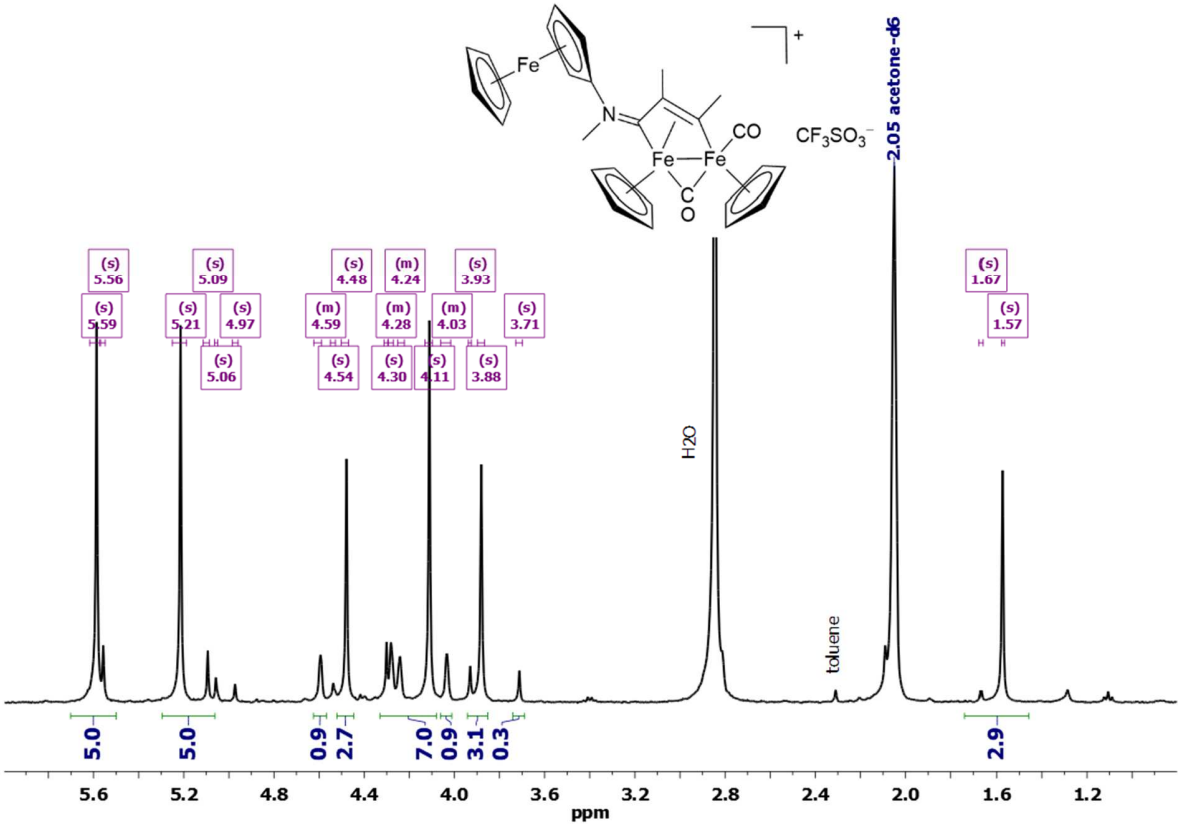

Figure S34. $^{13}C\{^{1}H\}$ NMR spectrum (101 MHz, acetone-d_6) of **5c** (*cis-E*/*Z* ratio = 7.6).

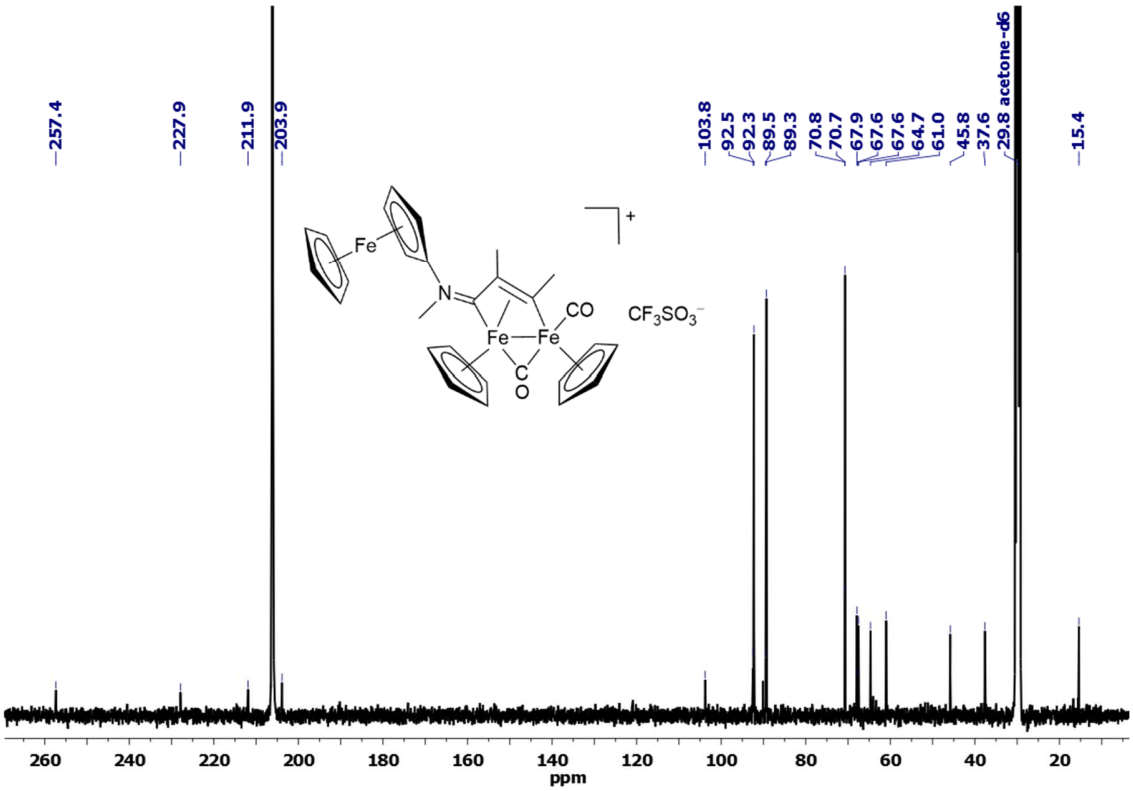

Figure S35. Black line: ^{1}H NMR spectrum (401 MHz, acetone-d_6) of **5c**. Blue line: ^{1}H NOESY with irradiation at 5.59 ppm (Cp of *cis-E*-**5c**). Red line: ^{1}H NOESY with irradiation at 5.21 ppm (Cp^{L} of *cis-E*-**5c**). Green line: ^{1}H NOESY with irradiation at 5.09 ppm (Cp^{L} of *cis-Z*-**5c**). NOEs are indicated by the arrows.

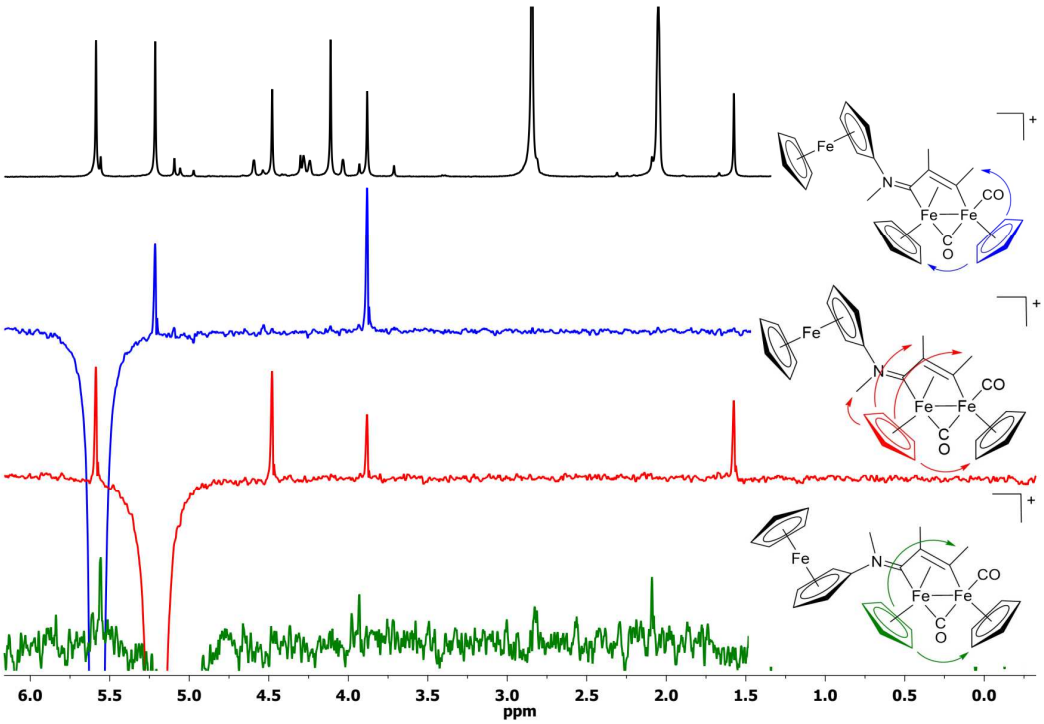

Figure S36. ^{1}H NMR spectrum (401 MHz, $CDCl_3$) of $[Fe_2Cp_2Cl(CO)_2\{\mu\text{-}CNMe(Fc)\}]$, **6** (*cis*-*E*/*Z* ratio = 1.5). Signals due to *trans* isomers are marked with asterisk (*).

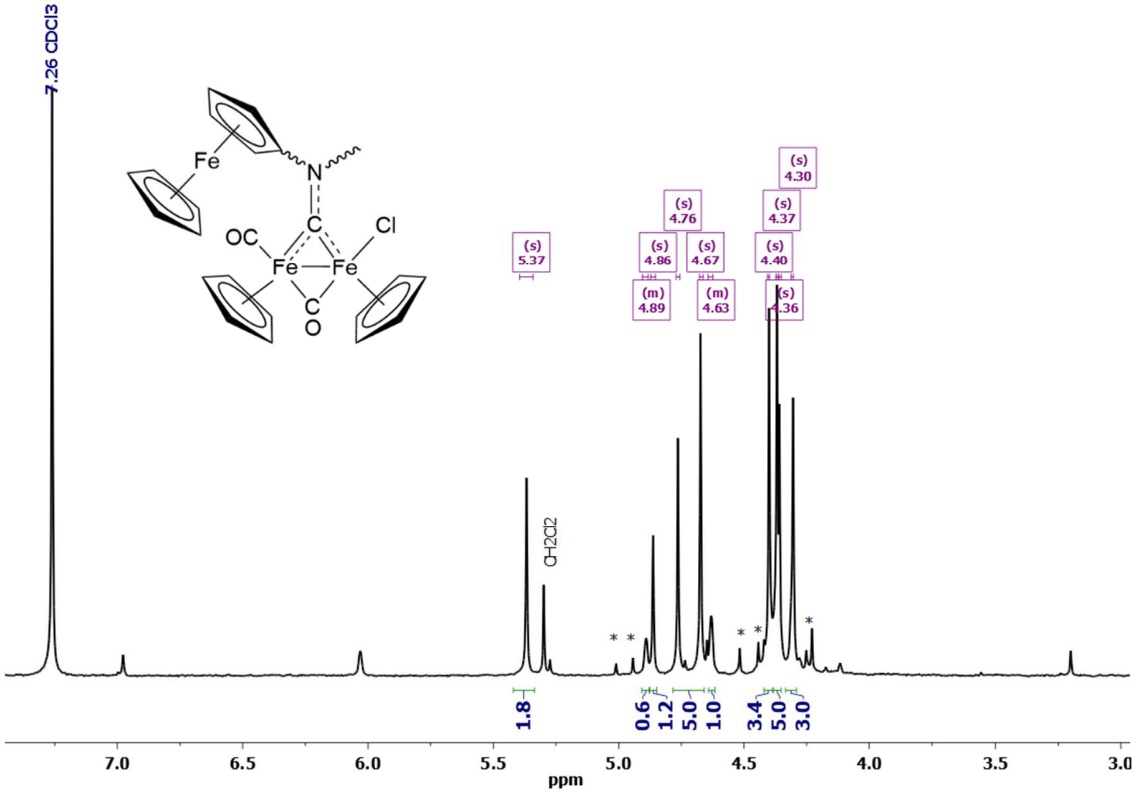

qNMR purity assessment

Figure S37. ^{1}H NMR spectrum (401 MHz, acetone-d_6) of **2** (*cis-E/Z* ratio = 1.8 + *ca.* 6 % *trans* isomers) + 1,3,5-trimethoxybenzene (standard for qNMR).

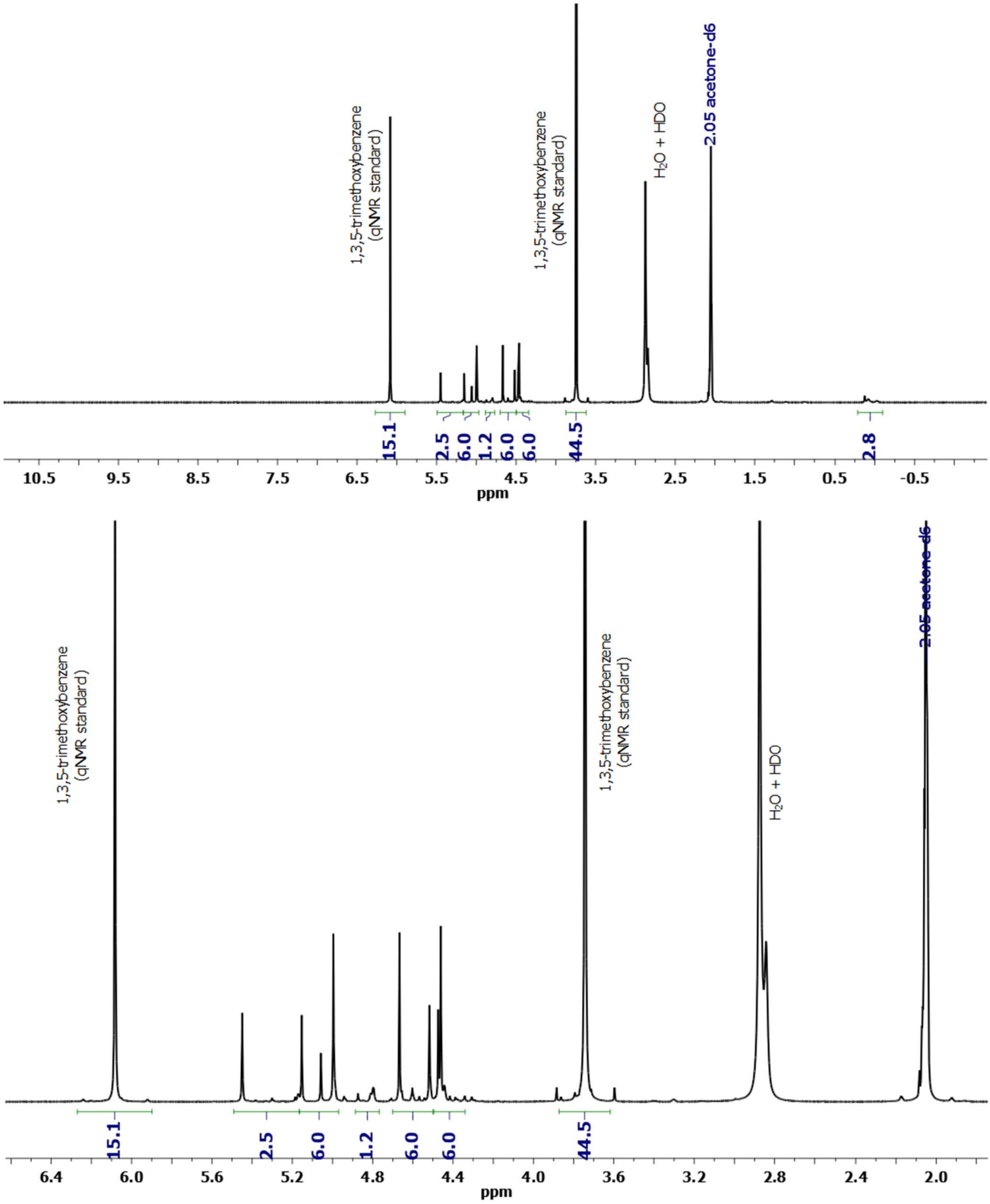

Figure S38. ^{1}H NMR spectrum (401 MHz, acetone-d_6) of **3a** (*cis-E/Z* ratio ≈ 1 + traces of *trans* isomers) + 1,3,5-trimethoxybenzene (standard for qNMR).

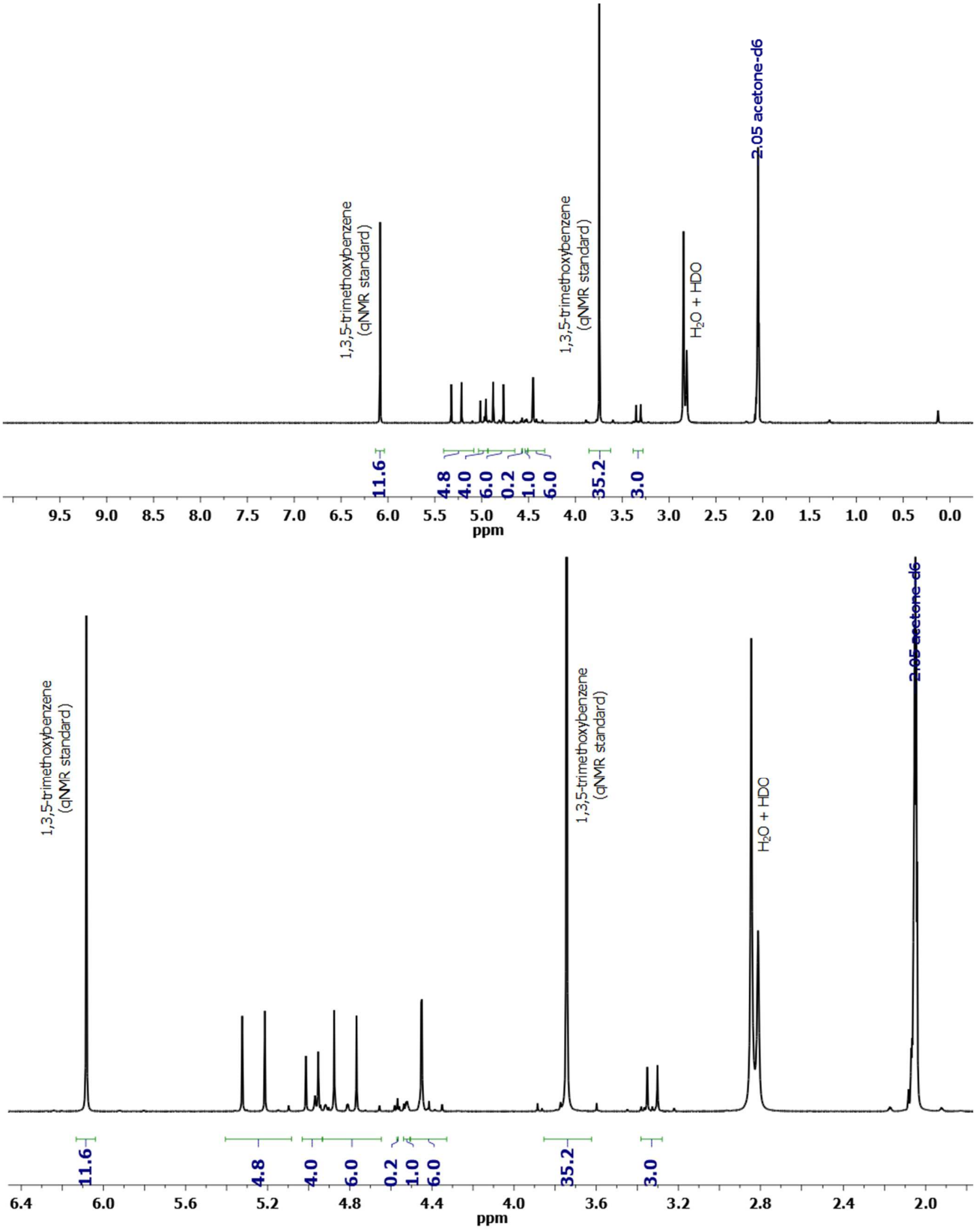

Figure S39. ^{1}H NMR spectrum (401 MHz, acetone-d_6) of **3b** (*cis*-*E*/*Z* ratio = 1.5 + *trans* isomer; *cis*/*trans* ratio = 4.1; signals marked with asterisk *) + 1,3,5-trimethoxybenzene (standard for qNMR).

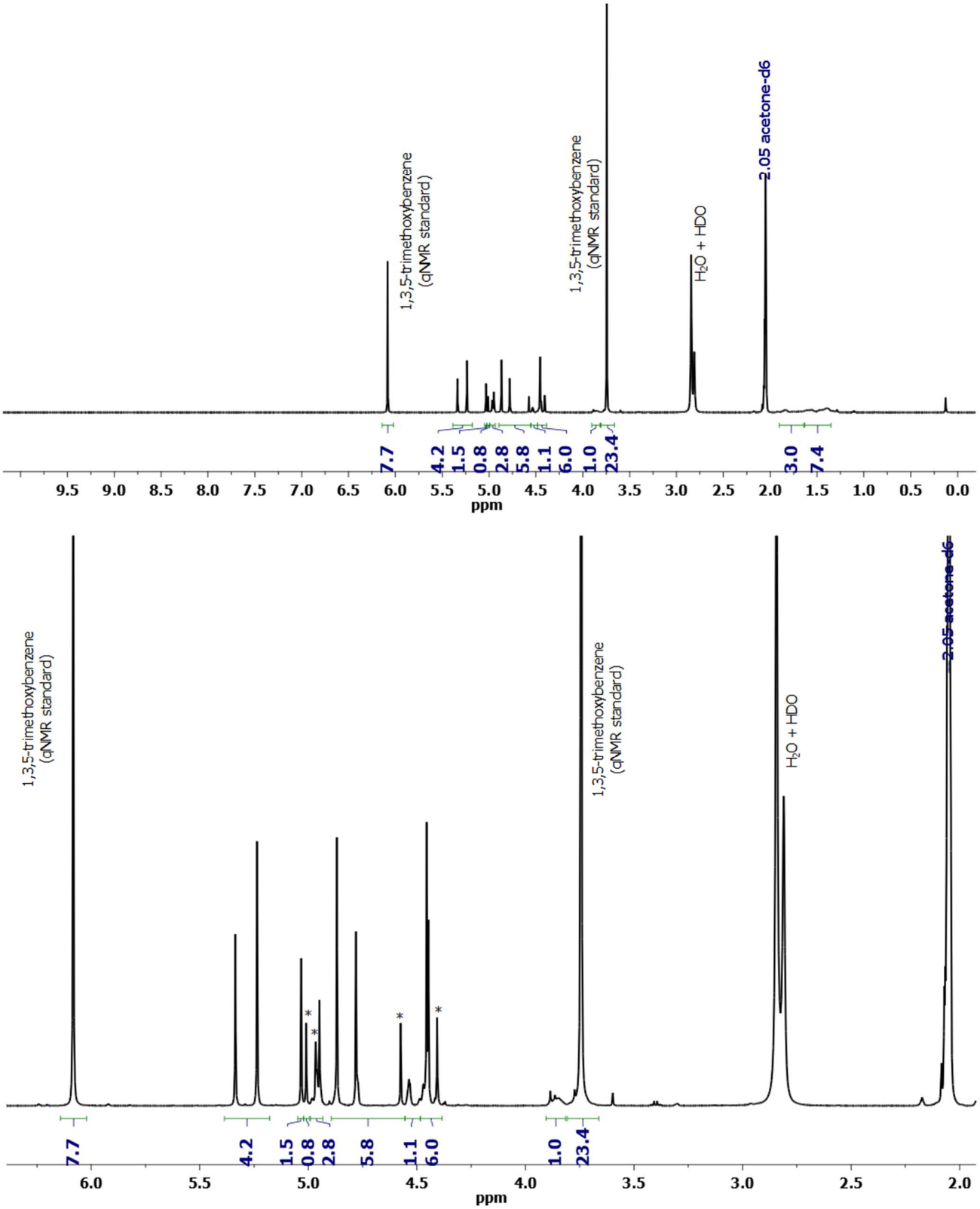

Figure S40. ^{1}H NMR spectrum (401 MHz, CD_3CN) of **5a** (*cis*-*E*/*Z* ratio = 2.2) + 1,3,5-trimethoxybenzene (standard for qNMR).

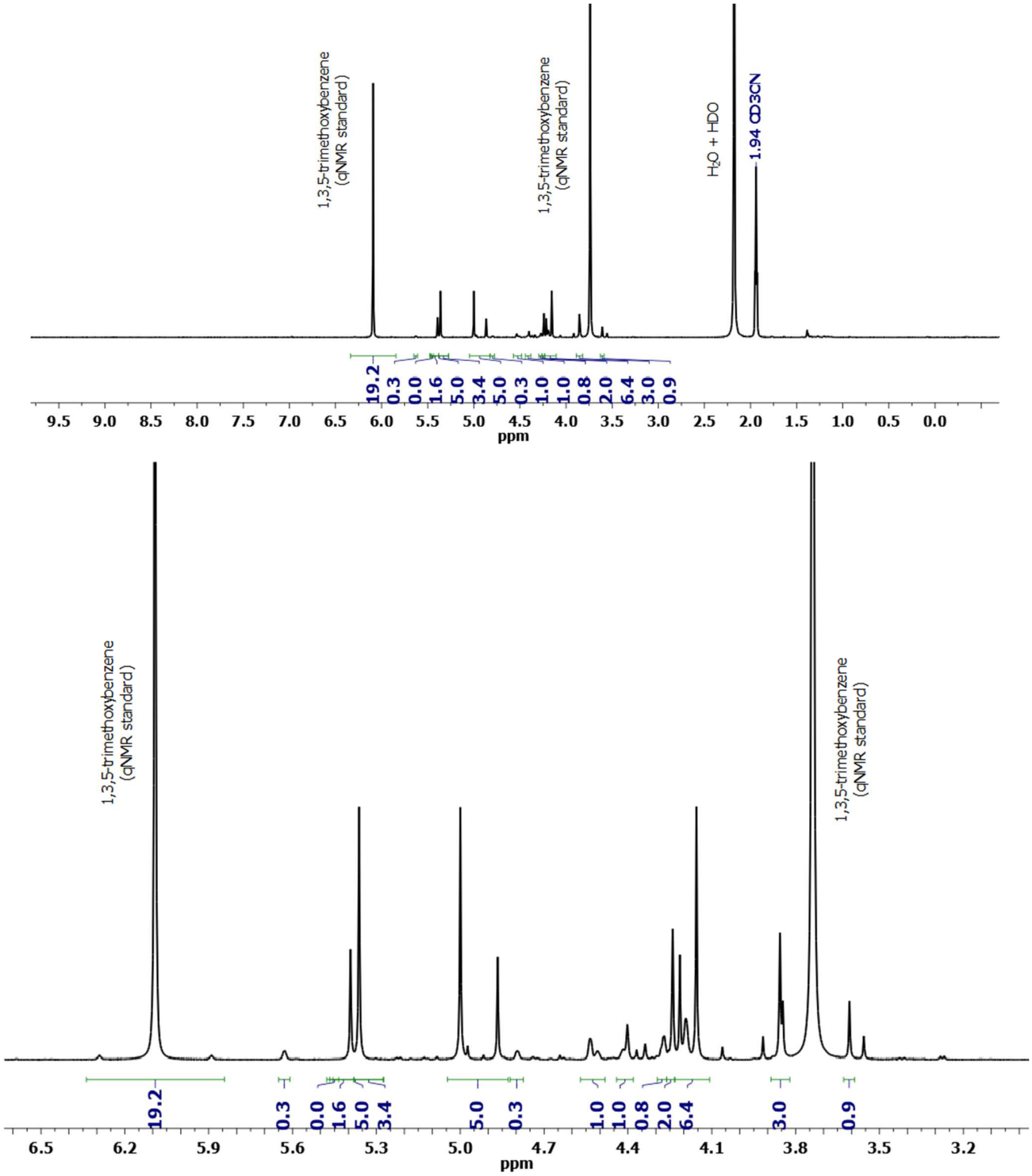

Figure S41. ^{1}H NMR spectrum (401 MHz, acetone-d_6) of **5b** (*cis-E*/*Z* ratio = 9.1; signals of *cis-Z*-**5b** are marked with asterisk *) + 1,3,5-trimethoxybenzene (standard for qNMR).

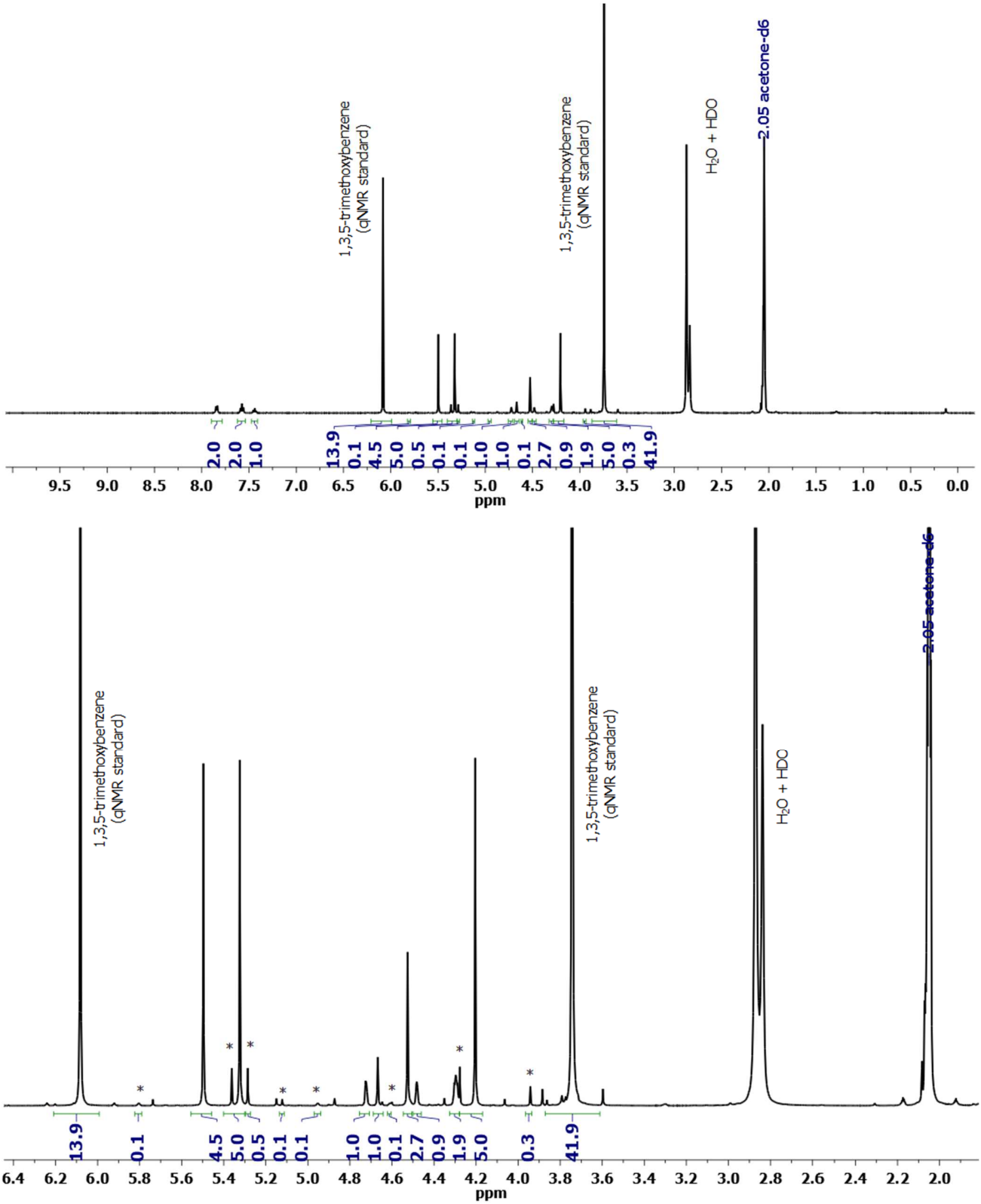

Figure S42. ^{1}H NMR spectrum (401 MHz, acetone-d_6) of **5c** (*cis-E*/*Z* ratio = 7.6) + 1,3,5-trimethoxybenzene (standard for qNMR). The N-Me resonance of the *cis-Z* isomer (marked with asterisk *) is partially superimposed to the OMe resonance of 1,3,5-trimethoxybenzene.

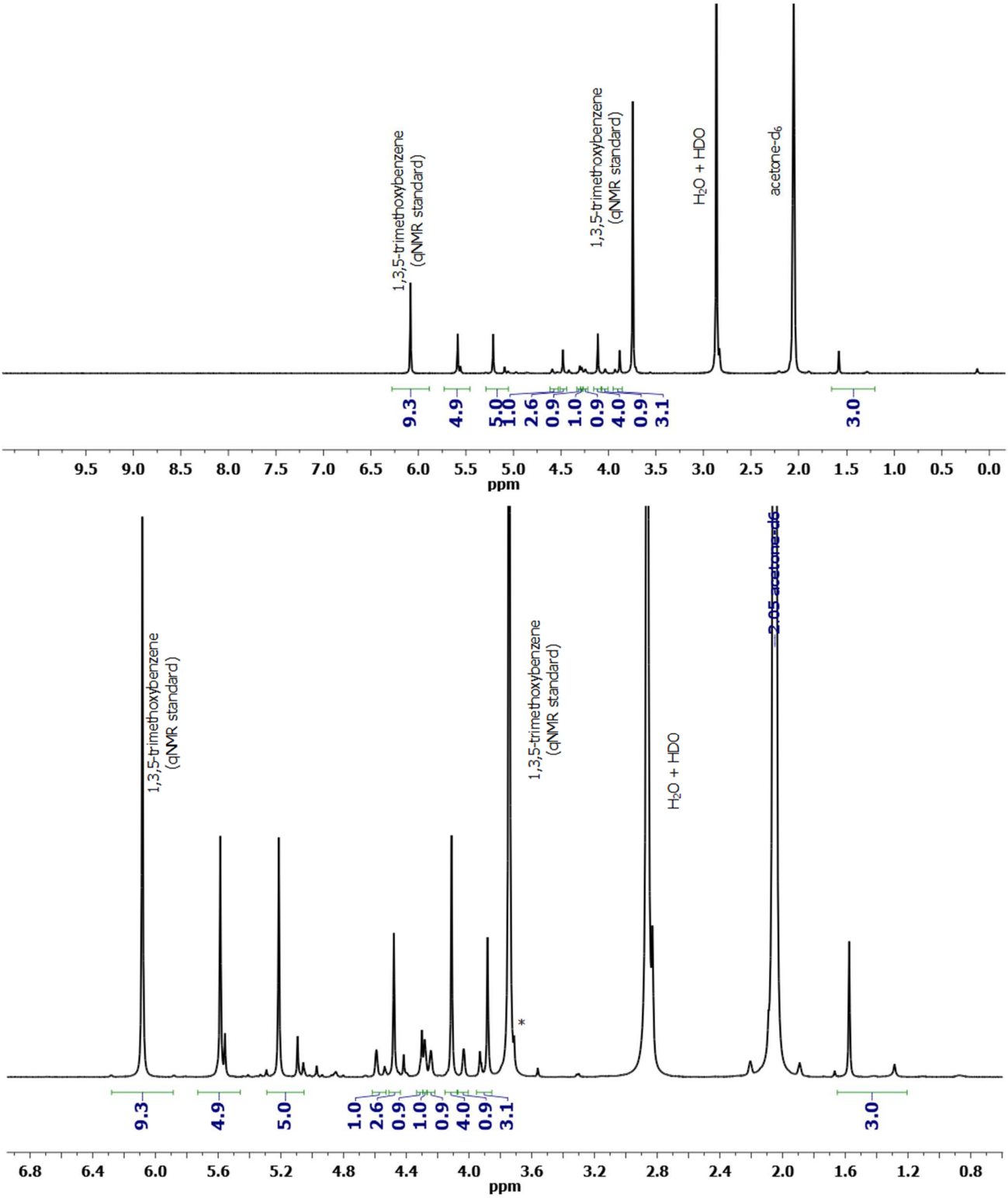

Table S1. Purity determination of **2**, **3a,b**, **5a-c** via qNMR analyses in acetone-d_6 or CD_3CN solution with 1,3,5-trimethoxybenzene as standard.

$$\%P_{Fe} = \frac{(I_{Fe}/N_{Fe})}{(I_{std}/N_{std})} \cdot \frac{(m_{std}/M_{std})}{(m_{Fe}/M_{Fe})} \cdot \%P_{std}$$

Fe compound (analyte)			1,3,5-trimethoxybenzene (standard)			NMR data Relative integrals (I) and corresponding number of protons (N)				Fe compound purity (%)
Sample	molar mass (g/mol)	mass (g)	molar mass (g/mol)	mass (g)	Purity (%)					
	m_{Fe}	M_{Fe}	m_{std}	M_{std}	$\%P_{std}$	I_{std}	N_{std}	I_{Fe}	N_{Fe}	$\%P_{Fe}$
2	690.073	2.046	168.19	2.347	99.8	44.52	9	6	6	95.0
3a	714.094	1.716	168.19	1.508	99.8	35.20	9	6	6	95.2
3b	781.203	2.705	168.19	1.442	99.8	23.40	9	6	6	95.0
5a	713.106	2.086	168.19	2.992	99.8	19.19	3	5	5	94.9
5b	775.175	2.047	168.19	1.97	99.8	41.91	9	5	5	95.1
5c	727.133	4.001	168.19	2.727	99.8	9.27	3	3	3	95.2

Table S2. Hydrogen bonds for *cis-E*-**5b**·H_2O [Å and °].

D-H···A	d(D-H)	d(H···A)	d(D···A)	<(DHA)
O(101)-H(111)···O(13)#1	0.88(2)	2.06(2)	2.923(4)	164(5)
O(101)-H(112)···O(12)#2	0.88(2)	2.11(2)	2.965(5)	165(5)

Symmetry transformations used to generate equivalent atoms:
#1 x+1, y, z; #2 -x+1, -y, -z+1.

Table S3. Crystal data and measurement details for *cis-E*-**3a**, *cis*-**4b** and *cis-E*-**5b**·H_2O.

	cis-E-**3a**	*cis*-**4b**	*cis-E*-**5b**·H_2O
Formula	$C_{27}H_{25}F_3Fe_3N_2O_5S$	$C_{38}H_{44}F_3Fe_3N_3O_4S$	$C_{33}H_{31}F_3Fe_3NO_6S$
FW	714.10	863.37	794.20
T, K	100(2)	100(2)	100(2)
λ, Å	0.71073	0.71073	0.71073
Crystal system	Monoclinic	Orthorhombic	Monoclinic
Space group	$P2_1/n$	$P2_12_12_1$	$P2_1/c$
a, Å	8.9391(3)	11.2389(7)	11.7307(3)
b, Å	18.5516(7)	16.8628(11)	11.0006(3)
c, Å	16.6455(6)	19.0064(12)	24.6106(6)
β,°	104.1780(10)	90	101.3380(10)
Cell Volume, Å^3	2676.32(17)	3602.1(4)	3113.89(14)
Z	4	4	4
D_c, g·cm^{-3}	1.772	1.592	1.694
μ, mm^{-1}	1.746	1.311	1.512
F(000)	1448	1784	1620
Crystal size, mm	0.18×0.15×0.12	0.16×0.14×0.11	0.15×0.12×0.09
θ limits,°	1.672-25.498	1.614-25.999	1.688-25.999
Reflections collected	36161	49721	43404
Independent reflections	4981 [R_{int} = 0.0278]	6997 [R_{int} = 0.0399]	6124 [R_{int} = 0.0564]
Data / restraints /parameters	4981 / 0 / 372	6997 / 0 / 471	6124 / 2 / 431
Goodness on fit on F^2 [a]	1.109	1.119	1.050
R_1 ($I > 2\sigma(I)$) [b]	0.0449	0.0282	0.0426
wR_2 (all data) [c]	0.1052	0.0718	0.1159
Largest diff. peak and hole, e Å^{-3}	1.447 / -0.740	0.656 / -0.264	1.715 / -1.269

[a] Goodness on fit on $F^2 = [\Sigma w(F_O^2 - F_C^2)^2/(N_{ref} - N_{param})]^{1/2}$, where $w = 1/[\sigma^2(F_O^2) + (aP)^2 + bP]$, where $P = (F_O^2 + 2F_C^2)/3$; N_{ref} = number of reflections used in the refinement; N_{param} = number of refined parameters. [b] $R_1 = \Sigma||F_O| - |F_C||/\Sigma|F_O|$. [c] $wR_2 = [\Sigma w(F_O^2 - F_C^2)^2/\Sigma w(F_O^2)^2]^{1/2}$, where $w = 1/[\sigma^2(F_O^2) + (aP)^2 + bP]$, where $P = (F_O^2 + 2F_C^2)/3$.

Simulated IR and NMR spectra

Figure S43. Simulated IR spectra of *cis* and *trans* isomers of **4a** (C-PCM/r^{2}SCAN-3c, acetone as continuous medium). Lorentzian broadening functions, FWHM = 8 cm^{-1}.

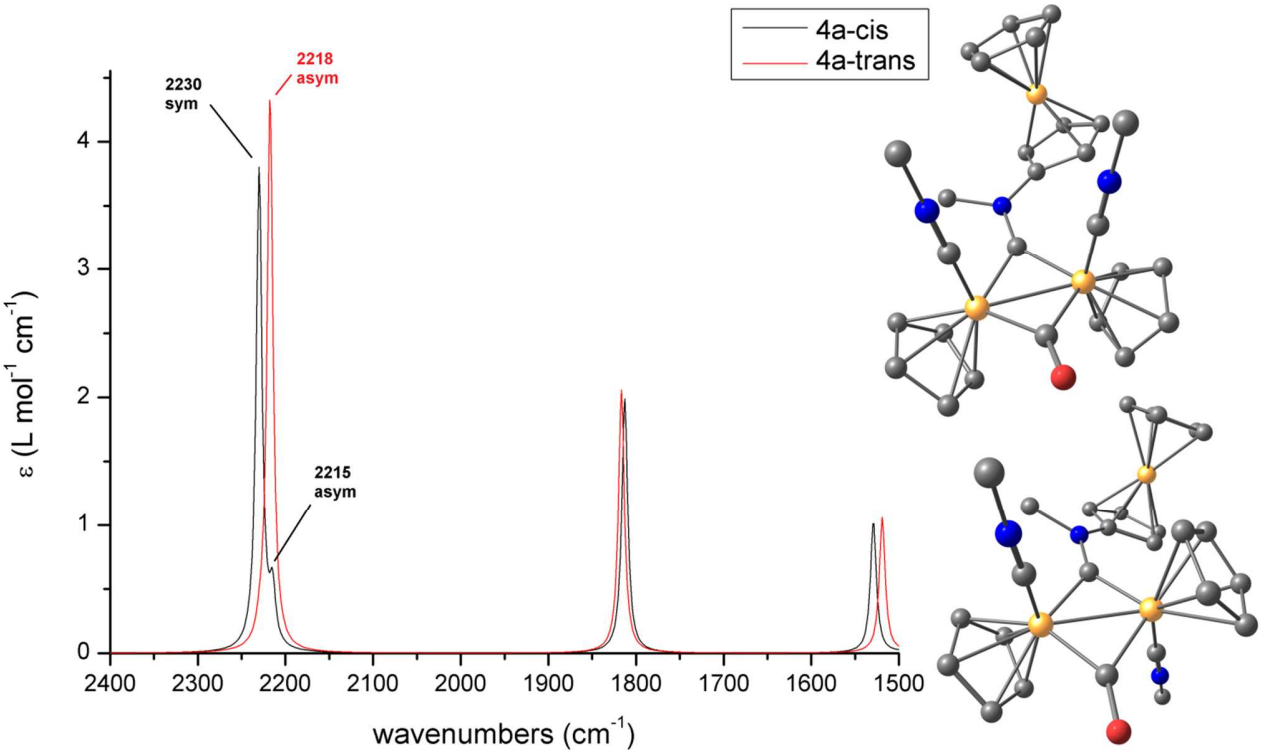

Figure S44. Simulated IR spectra of the isomers of **5c** (C-PCM/r²SCAN-3c, acetone as continuous medium). Lorentzian broadening functions, FWHM = 8 cm^{-1}.

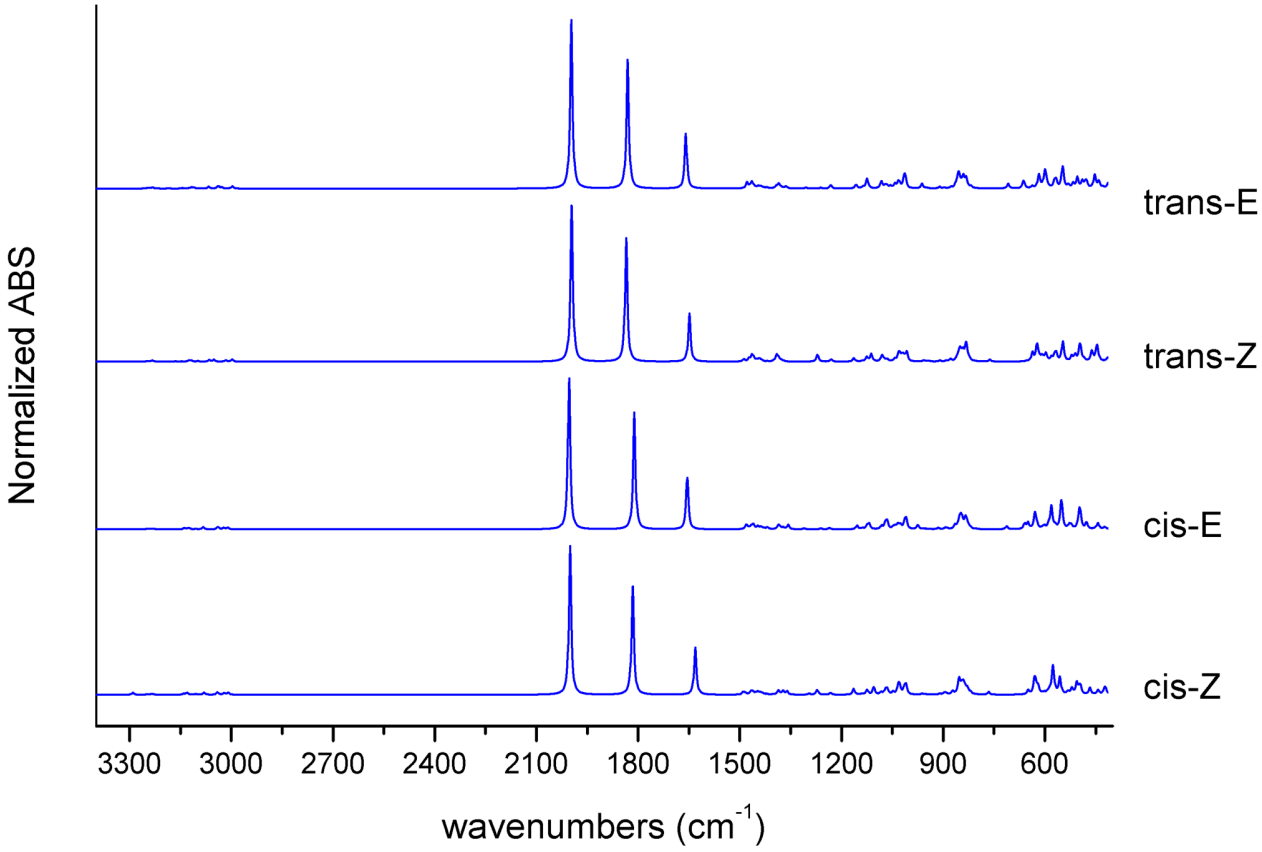

Figure S45. Simulated ^{1}H NMR spectra of *cis-E*-**5c** (top) and *cis-Z*-**5c** (bottom); experimental spectrum of **5c** (*cis-E*/*Z* ratio = 7.6) in acetone-d_6.

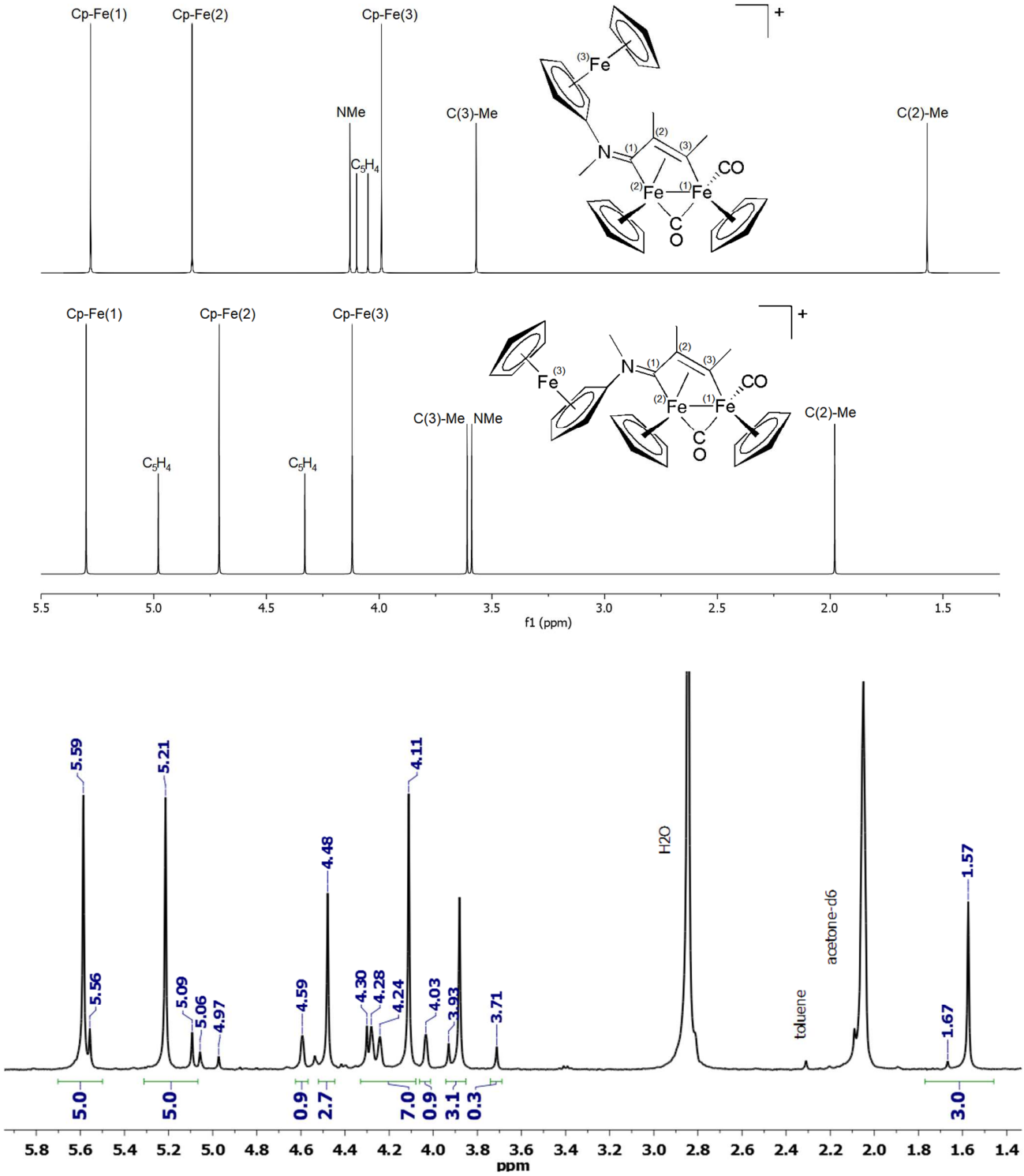

Figure S46. Simulated $^{13}C\{^{1}H\}$ NMR spectra of *cis-E*-**5c** (top) and *cis-Z*-**5c** (middle); experimental spectrum of **4c** (*cis-E*/*Z* ratio = 7.6) in acetone-d_6.

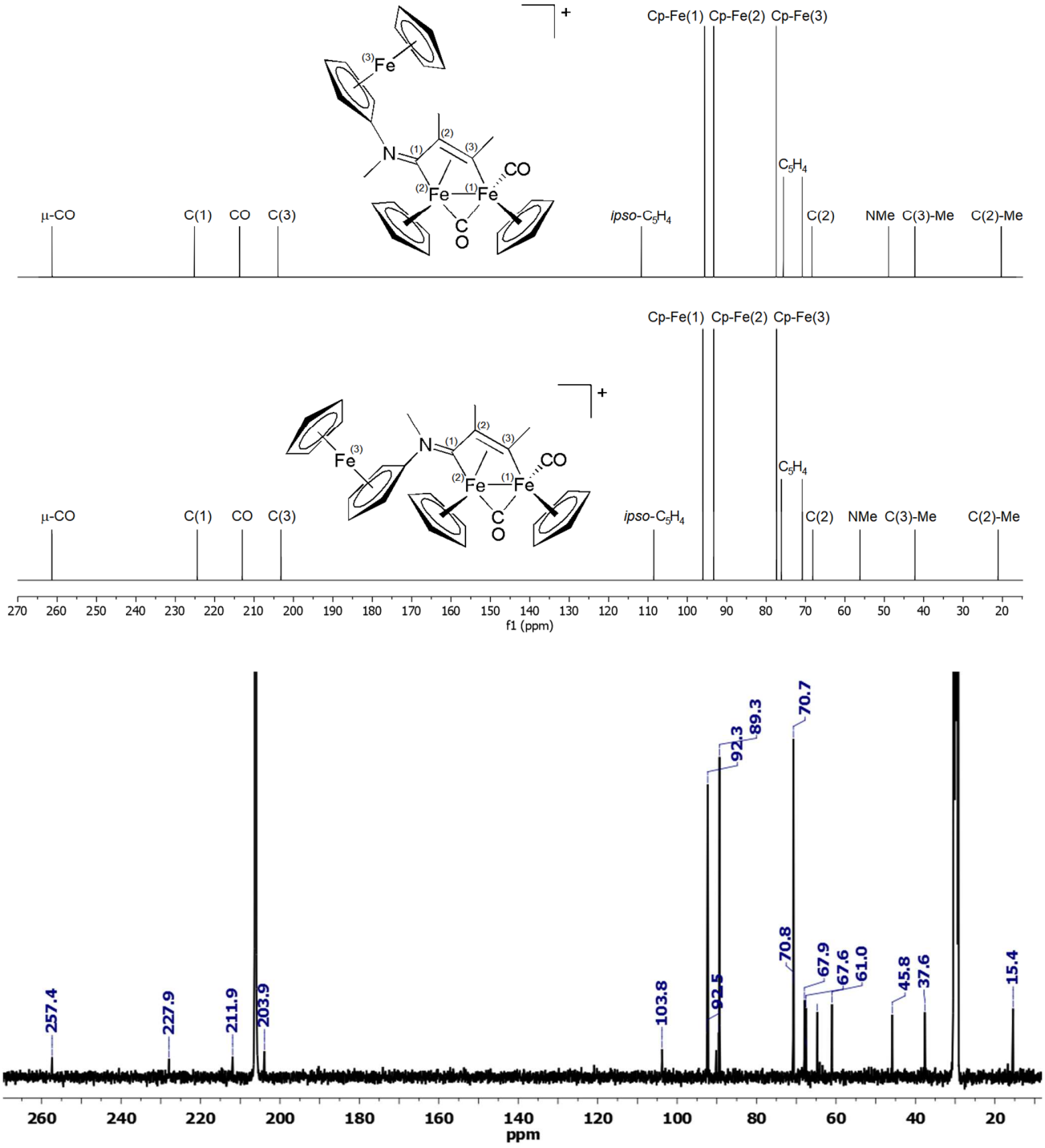

Cyclic voltammetry

Figure S47. Cyclic voltammetry of **5b** recorded at a Pt electrode in 0.2 M $[N^nBu_4]PF_6/CH_2Cl_2$ solution between –1.75 and +1.15 V (*vs* $FeCp_2$). Scan rate: 0.1 V/s.

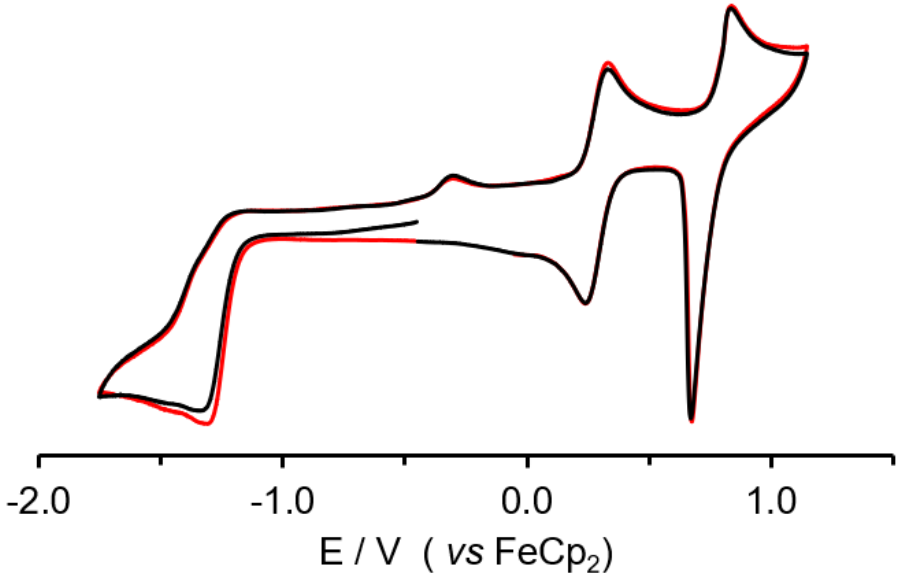

Figure S48. Cyclic voltammetries of **5b** recorded at a Pt electrode in 0.2 M $[N^nBu_4]PF_6/CH_2Cl_2$ solution (vs Ag/AgCl) between –1.75 and +0.55 V. Scan rate: 0.1 V/s (red line), 0.2 V/s (black line), 1 V/s (blue line).

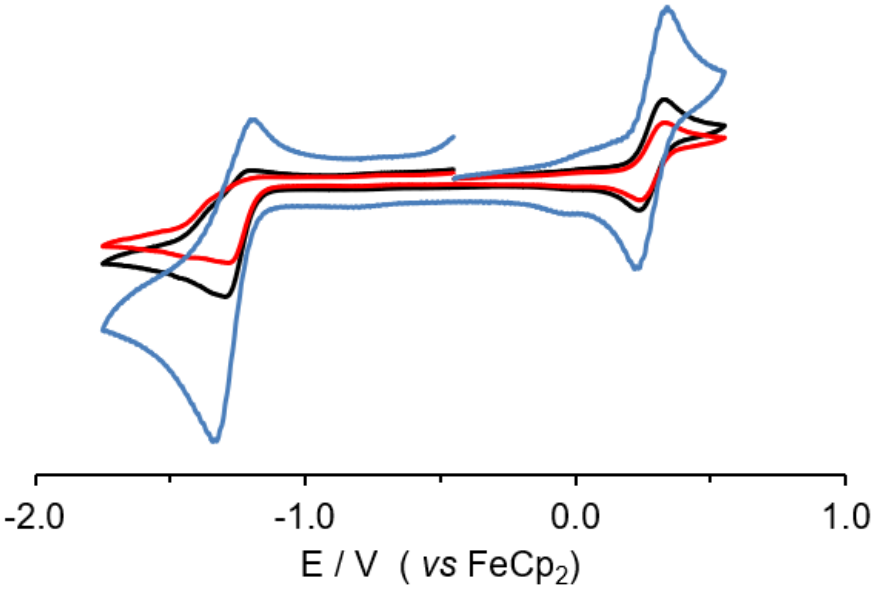

Cytotoxicity studies

Figure S49. Dose-response curves of distinct cell lines treated with the investigated triiron compounds.

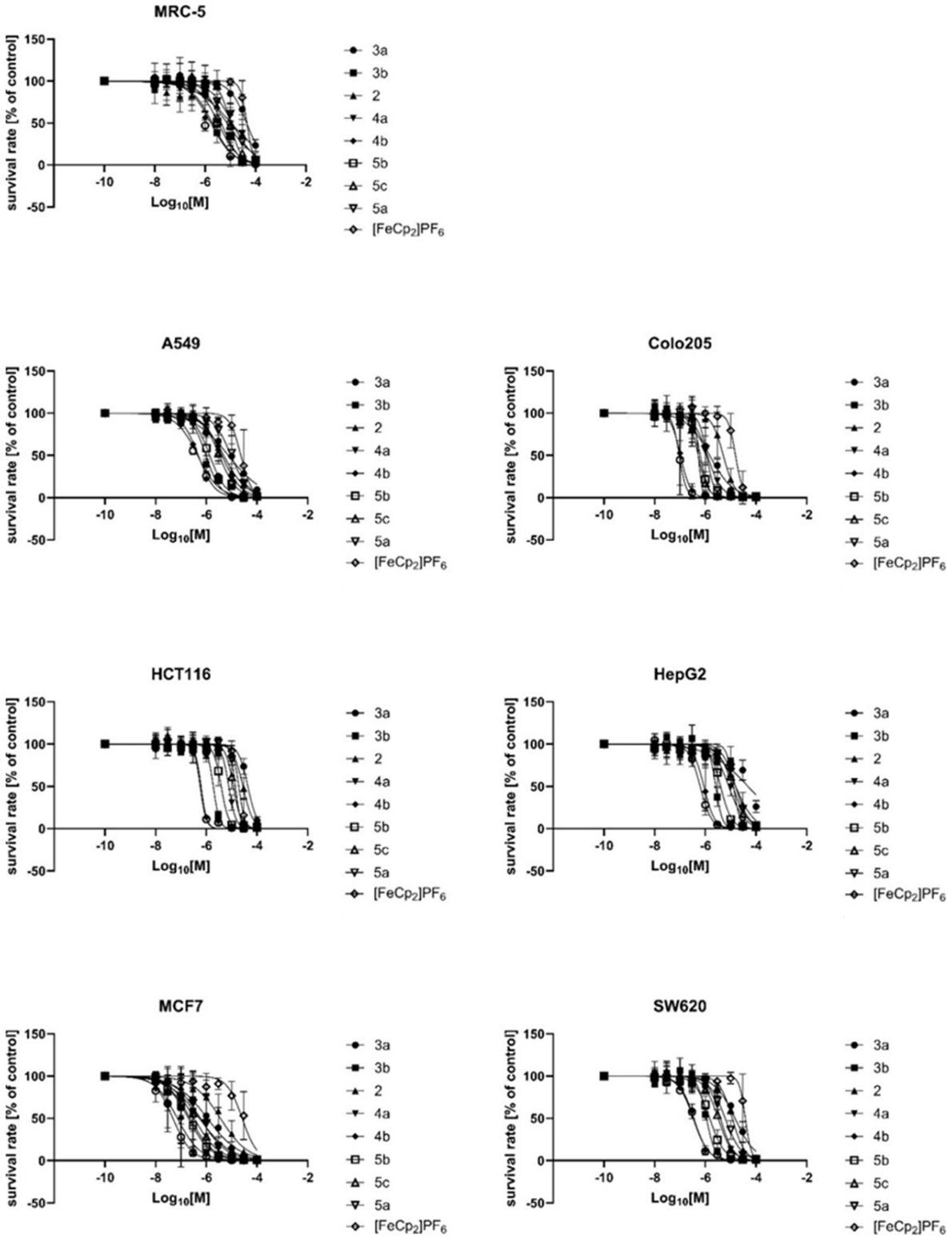

Figure S50. Correlation between Log P_{ow} values (vertical axis) and median IC_{50} values (μM, horizontal axis) of investigated triiron complexes.